Cellular/Molecular

Restricted Cortical and Amygdaloid Removal of Vesicular Glutamate Transporter 2 in Preadolescent Mice Impacts Dopaminergic Activity and Neuronal Circuitry of Higher Brain Function

Åsa Wallén-Mackenzie,[1] Karin Nordenankar,[1] Kim Fejgin,[4]* Malin C. Lagerström,[1]* Lina Emilsson,[1] Robert Fredriksson,[1] Caroline Wass,[4] Daniel Andersson,[4] Emil Egecioglu,[5] My Andersson,[5] Joakim Strandberg,[5] Örjan Lindhe,[6] Helgi B. Schiöth,[1] Karima Chergui,[7] Eric Hanse,[5] Bengt Långström,[2] Anders Fredriksson,[1] Lennart Svensson,[4] Erika Roman,[3] and Klas Kullander[1]

Departments of [1]Neuroscience, [2]Biochemistry and Organic Chemistry, and [3]Pharmaceutical Biosciences, Uppsala University, 751 24 Uppsala, Sweden, Departments of [4]Pharmacology and [5]Physiology, Göteborg University, 405 30 Göteborg, Sweden, [6]Uppsala Imanet, GE Healthcare, 751 09 Uppsala, Sweden, and [7]Department of Physiology and Pharmacology, Karolinska Institutet, 171 77 Stockholm, Sweden

A major challenge in neuroscience is to resolve the connection between gene functionality, neuronal circuits, and behavior. Most, if not all, neuronal circuits of the adult brain contain a glutamatergic component, the nature of which has been difficult to assess because of the vast cellular abundance of glutamate. In this study, we wanted to determine the role of a restricted subpopulation of glutamatergic neurons within the forebrain, the *Vglut2*-expressing neurons, in neuronal circuitry of higher brain function. *Vglut2* expression was selectively deleted in the cortex, hippocampus, and amygdala of preadolescent mice, which resulted in increased locomotor activity, altered social dominance and risk assessment, decreased sensorimotor gating, and impaired long-term spatial memory. Presynaptic VGLUT2-positive terminals were lost in the cortex, striatum, nucleus accumbens, and hippocampus, and a downstream effect on dopamine binding site availability in the striatum was evident. A connection between the induced late-onset, chronic reduction of glutamatergic neurotransmission and dopamine signaling within the circuitry was further substantiated by a partial attenuation of the deficits in sensorimotor gating by the dopamine-stabilizing antipsychotic drug aripiprazole and an increased sensitivity to amphetamine. Somewhat surprisingly, given the restricted expression of *Vglut2* in regions responsible for higher brain function, our analyses show that VGLUT2-mediated neurotransmission is required for certain aspects of cognitive, emotional, and social behavior. The present study provides support for the existence of a neurocircuitry that connects changes in VGLUT2-mediated neurotransmission to alterations in the dopaminergic system with schizophrenia-like behavioral deficits as a major outcome.

Key words: **neuronal network; physiology; CNS; transmitter; behavior; schizophrenia**

Introduction

All neuronal circuits of the nervous system contain an excitatory component, and the most common excitatory neurotransmitter in the adult nervous system is glutamate. The presence of glutamate in all cells, combined with the long-standing lack of presynaptic glutamatergic markers long hampered studies of the glutamatergic neuron itself, as well as its role in the neurocircuitry of specific functions.

Identified a few years back, vesicular glutamate transporters 1 and 2 (VGLUT1 and VGLUT2) are now recognized as reliable markers of glutamatergic neurons. The *Vglut1* (*Slc17a7*) and *Vglut2* (*Slc17a6*) genes are specifically expressed in glutamatergic neurons and are responsible for the vesicular packaging of glutamate in the presynaptic axon terminal (Bellocchio et al., 2000; Takamori et al., 2000, 2001; Fremeau et al., 2001; Herzog et al., 2001). In the adult mouse brain, the expression of *Vglut1* and *Vglut2* show a complementary and mainly reciprocal distribution, and together, the two transporters cover most of the established glutamatergic neurons (Fremeau et al., 2004a). *Vglut2* predominates in the thalamus, hypothalamus, deep cerebellar

Received Dec. 9, 2008; accepted Jan. 7, 2009.

This work was supported by Swedish Medical Research Council (SMRC) Grants K2004-32P-15230-01A and K2005-33X-15327-01A, the Foundations of Knut and Alice Wallenberg, Åke Wiberg, Magnus Bergwall, Uppsala University (K.K.), SMRC 4247 (J. Engel), Swedish Brain Foundation (Å.W.-M., M.C.L.), and Lundbeck Foundation (M.C.L.). Bristol-Myers Squibb, Sweden, generously supplied aripiprazole. K.K. is a Royal Swedish Academy of Sciences Research Fellow supported by a grant from the Knut and Alice Wallenberg Foundation. Prof. Meyerson is gratefully acknowledged for his guidance in the behavior tests used, especially the use of the multivariate concentric square field test. We thank I. Riebe, T. Abrahamsson, M. Berg, O. Eriksson, A. Nordin, A.-K. Olsson, A. Nygård, J. Dahlbom, O. Stephansson, H. Bengtsson, and the Uppsala University Transgenic Facility for excellent assistance. We are grateful to Dr. Fujiyama (Kyoto University, Kyoto, Japan) for the kind gift of VGLUT2 antibodies, to Dr. Arber for the Tau ^{mGFP} mice, and to Profs. T. Lewander and T. Perlmann for critical reading of this manuscript.

*K.F. and M.C.L. contributed equally to this work.

Correspondence should be addressed to Klas Kullander, Department of Neuroscience, Uppsala University, Box 593, 75124 Uppsala, Sweden. E-mail: klas.kullander@neuro.uu.se.

DOI:10.1523/JNEUROSCI.5851-08.2009

 0270-6474/09/292238-14$15.00/0

nuclei, certain amygdaloid nuclei, and brainstem (Fremeau et al., 2001; Herzog et al., 2001; Sakata-Haga et al., 2001; Kaneko and Fujiyama, 2002; Stornetta et al., 2002; Varoqui et al., 2002; Oliveira et al., 2003), whereas *Vglut1* predominates in the cerebral cortex and hippocampus, structures with only restricted *Vglut2* expression. The temporal onset of *Vglut1* and *Vglut2* expression differs in that *Vglut1* expression is upregulated around birth and peaks at 2 week of age, whereas *Vglut2* expression is widely distributed during embryogenesis, peaks at around birth, and subsequently becomes downregulated in cells in which *Vglut1* is progressively upregulated (Fremeau et al., 2004b). The difference in their expression patterns provides an explanation for the phenotypes observed in mice carrying targeted deletion of the *Vglut1* and *Vglut2* genes, respectively. *Vglut1*-null mutant mice are viable but suffer a progressive neurological phenotype that includes blindness and an enhanced startle response (Fremeau et al., 2004b; Wojcik et al., 2004). In contrast, *Vglut2*-null mutant mice die immediately after birth because of failure of the respiratory central pattern generator in the brainstem (Moechars et al., 2006; Wallén-Mackenzie et al., 2006). Thus, highly divergent roles for the VGLUT1 and VGLUT2 proteins are implied in the nervous system; however, because of the neonatal lethality of the *Vglut2* mutant mice, the role of VGLUT2-mediated neurotransmission in higher brain function is still unknown.

A putative role for dysregulated glutamate neurotransmission in diseases of mental processes has been recognized since the discovery that phencyclidine (PCP), a noncompetitive inhibitor of the NMDA glutamate receptors, could induce a psychotic state in humans that was very similar to schizophrenia (Luby et al., 1959; Allen and Young, 1978). This complex disease is characterized by positive symptoms, such as hallucinations and thought disorder, negative symptoms that include blunted affect and deficits in social behavior, and symptoms of cognitive dysfunction, such as deficits in memory, attention, and problem solving (Lewis and Lieberman, 2000; Tamminga and Holcomb, 2005). The classical model for explaining schizophrenia, the so-called dopamine hypothesis of schizophrenia, which suggests a subcortical dopaminergic hyperactivity, is based on the fact that a majority of antipsychotic drugs used to treat schizophrenia target the dopamine D_2 receptors (Seeman et al., 1976).

In this study, we deleted *Vglut2* during the third postnatal week in the cortex, hippocampus, and amygdala of mice with the purpose of investigating whether VGLUT2-mediated neurotransmission has a role in neuronal circuitry of higher brain function despite its limited expression in forebrain areas.

Materials and Methods

Generation of Vglut2-null animals. The *Vglut2* targeting construct and genotyping of mice was performed as previously published (Wallén-Mackenzie et al., 2006). $Vglut2^{f/f}$ mice were crossed to *nestin*-Cre and CaMKIIα-Cre mice (Minichiello et al., 1999) to generate mutant mice with specific forebrain deletion of VGLUT2 ($Vglut2^{f/f;nestin\text{-}Cre}$ and $Vglut2^{f/f;CaMKII\text{-}Cre}$). Male *nestin*-Cre mice were used for breeding to ensure promoter-specific expression of Cre. The appropriate local Swedish ethical committees have approved all experiments involving live animals (Permissions C156/4, C284/6, 285/2006).

In situ *hybridization histochemistry.* Floating *in situ* hybridization was performed as described previously (Lagerström et al., 2007). The *Vglut2* probe covers nucleotides 1616–2203 (NCBI accession number NM_080853.2), *Vglut1* probe covers 462–1067 (NM_182993), *VIAAT* covers 1578–1889 (NM_009508.1), *TH* covers 1300–1726 (NM_009377.1), and *DRD2* covers 2093–2545 (NM_010077.1).

Immunofluorescence histochemistry. Immunofluorescence was performed as described previously (Wallén-Mackenzie et al., 2006). Stacks of confocal images were analyzed using the three-dimensional image software Volocity (Improvision). To exclude background, volumes with intensities ranging from 1.5 to 19 SDs were counted and measured. Volumes smaller than 0.034, 0.037, and 0.39 μm^3 were excluded for striatum and hippocampus, cortex, and cerebellum, respectively. For dorsolateral striatum (bregma, 1.1–0.22) and nucleus accumbens (bregma, 1.1–0.74), each measured volume was 0.3×10^5; for cortex (bregma, 1.46–1.94 mm), each measured volume was 1×10^4; for cerebellum (bregma, −5.68 to −6.0 mm) and hippocampus (bregma, −1.46–1.94 mm), each measured volume was 1×10^5 μm^3, and six, nine, nine, three, and three volumes were measured per animal. In cerebellum, one measured area was in lobus flocculus, and two measured areas were in the cerebellar lobus 2. Two animals per genotype were used.

Quantitative real-time PCR. Mouse mRNA was extracted from brain tissues and converted into cDNA as previously described (Haitina et al., 2007). Quantitative real-time PCR was used to analyze differences in expression levels between $Vglut2^{f/f;CaMKII\text{-}Cre}$ mice and controls. All expression data were analyzed in duplicates, compensated for differences in primer efficiencies, and normalized against at least three stable housekeeping genes as previously described (Lindblom et al., 2006). The Grubbs test was used to identify and remove outliers. Differences in gene expression between groups were analyzed with the Mann–Whitney *U* test.

Prepulse inhibition of the acoustic startle. Acoustic startle was recorded by a MOPS 3 startle response recording system (Metod och Produkt; Svenska AB). The animals were placed in small Plexiglas cages ($10 \times 5.5 \times 5.5$ cm), which were suspended by a piston connected to a piezoelectrical sensor in a dimly lit and sound-attenuated cabinet ($52 \times 42 \times 38$ cm). A sudden movement of the animal inside the cage caused a displacement of the piston, thereby producing a signal detected by a connected microcomputer. The acoustic signal consisted of white noise delivered to the animal by two high-frequency loudspeakers built into the ceiling of the cabinet. A continuous acoustic signal provided a background white noise level of 62 dB(A) inside the cabinet. This signal was interrupted at stimulus presentations by a burst of white noise with a rise/decay time of 1 ms. Startle pulse intensity was set to 105 dB(A) and the prepulse intensities used were 68, 71, and 74 dB(A). Startle pulse duration was set to 20 ms, and prepulse duration was set to 20 ms. The prepulse was separated from the startle pulse by a delay of 40 ms. After an 8 min adaptation period with only background noise, the mice were subjected to five consecutive startle pulses, which were omitted from the analysis. Thereafter, the mice were presented with trials from three categories: startle pulse alone (3×15), prepulse alone (3 for each prepulse intensity), and prepulse plus startle pulse (15 for each prepulse intensity) in a pseudorandomized order. The individual trials were separated by intervals of varying length (5–15 s) and the total time of the test was 23 min including the adaptation period. The mean response amplitudes for pulse-alone (*P*) and prepulse plus pulse (*PP*) trials were calculated for each mouse and used to express the percentage prepulse inhibition according to the following formula: Prepulse inhibition (%) = $100 - ((PP/P) * 100)$.

A subset of the mice were tested first without treatment and then tested again the next day after systemic (intraperitoneal) administration with aripiprazole ($2.5 \text{ mg} \cdot \text{kg}^{-1}$). Aripiprazole was given 15 min before the start of the test. Phencyclidine ($5 \text{ mg} \cdot \text{kg}^{-1}$) was administered to a subset of animals exactly as above with the exception that the injection was given 5 min before the start of the test.

Social behavior. The social dominance tube test (Lindzey et al., 1961) and the social interaction test (File, 1980) was used to assess social behavior. In the tube test, a control littermate and a mutant mouse of the same sex were placed at opposite ends of a 30-cm-long and 3.5-cm-diameter tube and released. A subject was declared a "winner" when its opponent backed out of the tube. Each pairing was performed twice. For the social interaction test, male and female mice were housed in groups and tested individually in a social interaction paradigm by placing them in a novel arena (40×25 cm). Tests were performed between 9:00 and 11:00 A.M., and luminosity was maintained at 5–7 lux. The test subject was placed together with a sex-matched NMRI mouse and was free to interact for a 10 min period. Interaction time and number of interactions

were recorded and scored by a single observer blind to the genotype of the subject. Mounting, grooming, sniffing, fighting, and following were considered as interaction. For the second set of experiments, the same pair of animals (NMRI mouse and test subject) was reunited under the same conditions 48 h after the first interaction.

Morris water maze. A water maze paradigm modified after that of Morris (1984) was used to study spatial learning and long-term memory. The maze consisted of a circular pool with a diameter of 1.4 m and a circular Plexiglas escape platform (HVS Image) with a diameter of 10 cm. The pool was filled with water of a temperature of 24 ± 1°C, and the water surface was kept 1 cm above the platform. The mice were given an acclimatization training session in the water maze for 30 s during which the platform was removed. Two days later, a 6 d acquisition training began. The platform position was held constant throughout the 6 acquisition days, and the starting positions were randomized. An acquisition session consisted of five consecutive swims, each swim lasting a maximum of 60 s followed by a 30 s platform rest. The mean of each acquisition session was calculated and plotted. Long-term memory was assessed 48 h after the last day of acquisition by removing the platform and allowing animals to search the pool for 60 s (probe test). Data recordings were made using the 2020 Plus Tracking System (HVS Image), and learning was defined as mean time to find the platform during acquisition and long-term memory was defined as cumulative distance to previous platform position during the probe test, according to the Gallagher cumulative distance to platform (Gallagher et al., 1993).

The multivariate concentric square field. The multivariate concentric square field (MCSF) test is designed to include opportunity for exploration, risk assessment, risk taking, shelter seeking, and approach and avoidance behavior in rodents. The guiding principle for the MCSF test is that it is unprejudiced (i.e., the test is not designed to measure a particular mental condition). In one and the same trial, the animal is exposed to a free choice of different environmental settings and items that provide the opportunity to detect essential features of the animal's mentality. In this way, a behavioral profile is generated (Meyerson et al. 2006). The total arena area is 72 × 72 cm, divided into a central field (CENTER) (40 × 40 cm) and a peripheral corridor area 15 cm wide. The arena is built in black PVC (4 mm thick) with the exception of the outer wall of the BRIDGE area that was made of clear Plexiglas. The walls in the arena are 25 cm high with the exception of the walls surrounding the bridge that were 40 cm high. Within the central arena, a circular zone (CENTRAL CIRCLE) was defined. The zones CENTRAL SQUARE and CENTRAL CIRCLE were added into a cumulative zone named TOT CENTRE. From the central arena, the mice could enter three different corridors (EAST, SOUTH, WEST) through holes (diameter, 8 cm) in the central arena walls. The data from the three different corridors were added into one cumulative category named TOT CORR. The southeastern corner area was closed off by walls and covered with a black lid, thereby providing a dark corner room (DCR) (18 × 18 cm). The mice could enter the room from the east corridor side through a hole in the wall (8 cm). The southwestern corner area was closed off by walls to create the HURDLE room (18 × 18 cm) to which the mice had to climb through a hole situated 8 cm above the floor from either one of the adjacent corridors. A bridge structure was situated in the northern corridor. The bridge had slopes covered with a gray ribbed rubber mat, whereas the actual bridge (BRIDGE) consisted of a metal grid. The bridge was illuminated by a 40 W light source (125–190 lux) and led over a 45 cm gap. It could be climbed from two sides (SLOPE EAST and SLOPE WEST). The two slope zones were added into one cumulative category named TOT SLOPE. The test was performed by releasing the mouse in the central arena outside the CENTRAL CIRCLE. The mouse was allowed to explore the apparatus for 20 min. Between the testing of each animal, the bridge and slope area were washed with soapy water. The test was performed in dimly lit conditions (DCR, <1; CENTRE, 30; CORRIDORS, 10–15) with the exception of the bridge area. The test was videotaped and analyzed manually for latency (LAT), frequency (FRQ), and duration (DUR) to previously assigned zones. This MCSF and the functional interpretation of the various parameters generated have also been described in detail previously (Meyerson et al., 2006; Roman et al., 2006). The nonparametric Mann–Whitney *U* test was used for comparisons between *Vglut2*$^{f/f;CaMKII\text{-}Cre}$ and control mice, and the nonparametric Wilcoxon signed rank test was used for time resolution analysis. The StatView 5.0.1 (SAS Institute) software was used for the statistical analysis.

Elevated plus maze. The elevated plus maze (EPM) consisted of four arms, each 40 cm long and 10 cm wide, arranged in the shape of a plus sign and elevated 51 cm over the floor. Two opposite arms were open, whereas the other two were closed with 40-cm-high walls. The area inside the center of the EPM (10 × 10 cm) was not considered being either an open or closed arm. The EPM was made of black painted aluminum with a light rubber mat covering the floor. The animal was placed in the center of the EPM facing an open arm. Each animal was tested for 10 min under dimmed light. After each animal, the EPM was wiped clean with an ethanol solution and sufficient time was allowed for the apparatus to dry before the next animal was placed in the maze. The following parameters were scored: latency to first enter an open or closed arm as well as the frequency and duration of visits into the open and closed arms and the center portion. The behaviors were monitored by a TV–video setup. For the scoring, the open arm was split into an inner and an open part. The following parameters were scored manually by clocking the animal: latency (in seconds) to first enter an inner or outer open or closed arm as well as the frequency and duration (in seconds) of visits into the inner and outer open and closed arms and the center portion. To be scored as a visit, the animal's both hindlegs should have entered the section.

Total activity. Mice were housed individually in plastic cages in a room with an ambient temperature of 22°C and a 12 h light/dark cycle. The animals were tested between 8:00 A.M. and 1:00 P.M., under the same light and temperature conditions as in their cages. Ten mice were randomly chosen from each treatment group and drugs were administered by subcutaneous injections. Motor activity was measured during a 60 min period in an automated device consisting of a crate in which home cages (40 × 25 × 15 cm) were placed (Fredriksson et al., 1997). All types of vibration within the test cage [i.e., those caused by mouse movements, shaking (tremors), and grooming] were registered by a gramophone-like pick-up mounted horizontally with a counterweight, connected to the test cage.

Porsolt test. We used a modification of the method described by Porsolt et al. (1977). Mice were placed in a Plexiglass cylinder filled with water 25 cm deep to prevent animals from touching the bottom of the container with their tail. The water temperature was kept at 25°C to avoid temperature-related stress responses. Active time was defined as time spent swimming with at least three paws paddling. A mouse was considered inactive when floating and making only the movements necessary to keep its nostrils above the water. Behavior was recorded and analyzed blindly in two trials (trial 1 and trial 2) for 12 min per trial, and the active time was then expressed as swimming time. The potential between-group differences in activity/inactivity time were analyzed with a one-way ANOVA.

Frozen section autoradiography. [^{11}C]Raclopride was produced and delivered in a sterile buffered solution at >95% radiochemical purity according to a modified literature procedure following Uppsala Imanet, GE Healthcare, Standard Manufacturing Procedure. Frozen brain sections (20 mm) were prepared in a cryomicrotome and put on Superfrost glass slides. The slides were kept in a freezer (−20°C) until used. At the start of the experiment, the slides were preincubated at room temperature for 10 min in Tris+ buffer (50 mM Tris plus 120 mM NaCl plus 5 mM KCl plus 1 mM $MgCl_2$ plus 2.5 mM $CaCl_2$, pH 7.4). The slides were then transferred to containers containing 3 nM [^{11}C]raclopride in Tris+ buffer. In a duplicate set of containers, 1 μM unlabeled raclopride was added to block specific binding. After incubation for 30 min, the slides were washed three times for 3 min each time in buffer (0°C). The slides were dried in a heated (37°C) oven and exposed to phosphorimaging plates (GE Healthcare) for 40 min and scanned in a PhosphorImager model 400S (purchased from GE Healthcare). Regions of interest were drawn around the striatal area and quantified using ImageQuant, version 5.1 (GE Healthcare).

PET experiments. The animal was placed in a cylinder connected to an isoflurane vaporizer adjusted to deliver 3.8% isoflurane in a 40/60% mixture of oxygen and air. When the animal was unconscious, the concentration of isoflurane was reduced to 2.2%. A heparinized catheter

(Venflon GA) was placed in the tail vein and connected to a 1 ml syringe with 0.9% NaCl. The animal was subsequently placed on the camera bed on a water-heated mat (38°C) and covered to reduce the loss of body temperature during the experiment with its abdomen down and hindlegs stretched out backward. The tracer was injected as a bolus dose 10 s after the camera start in a volume of ~100 μl followed by 100 μl of saline. Imaging was performed on a microPET R4 scanner (Concorde Microsystems), with a computer-controlled bed and 10 cm transaxial and 8 cm axial field of view. It operates exclusively in three-dimensional list mode and has no septa. All raw data were first sorted into three-dimensional sinograms, followed by Fourier rebinning and two-dimensional filtered backprojection image reconstruction resulting in images with 2 mm^3 voxel resolution. Scatter correction, random counts, and dead time correction were all incorporated into the reconstruction algorithm. The acquisition time for the blank scan was 5 h and the 20 min transmission scan was generated with a spiraling point source containing 68Ge/68Ga (18.5 MBq) before injection of the tracer to correct the ensuing emission scan for attenuation scan. The time frames for the emission acquisition were as follows: 10 × 30 s, 5 × 120 s, and 5 × 300 s (duration, 40 min; 20 frames). Regions of interest were drawn around the striatal area and cerebellum and TACT curves were generated using ASIPro VM, version 6.3.3.0, and the quotient striatum/cerebellum was calculated to normalize for injected dose fluctuations and body weight. The amount of the injected activity was approx 2.5 MBq/mouse. Pharmacokinetic curves representing the radioactivity concentrations were calculated as activity in organ (in kilobecquerels per milliliter).

Biochemical quantification of dopamine content. After cervical dislocation, the striata from *Vglut2*$^{f/f;CaMKII\text{-}Cre}$ mice and littermate controls ($n = 22$ per genotype) were rapidly dissected on ice. The pieces were placed in preweighed tubes and used for subsequent analysis by HPLC using electrochemical detection (HPLC-ED). After ultrasound homogenization (Sonifier Cell Disruptor B30; Branson Sonic Power) in 0.1 M perchloric acid with 2.5 mM Na_2EDTA and subsequent centrifugation, dopamine content in homogenates was determined by HPLC-ED. Reverse phase with ion pair binding was used, and the resulting currents were analyzed by Dionex Chromeleon software (Dionex). Sample separation was performed over two Luna $C_{18}(2)$ 3 μm columns (Phenomenex; mobile phase of 5 mM citric acid, 10 mM sodium citrate, 10% acetonitrile, 4% tetrahydrofurane, and 10 mM Na_2EDTA, with or without 1-dodecanesulfonate), and amine content was detected by an amperometric detector (Waters 460; Millipore Waters).

Statistical analysis. Data were analyzed using unpaired two-tailed *t* test or one-way ANOVA with Bonferroni's *post hoc* comparisons unless otherwise stated. Values in graphs were expressed as mean ± SEM.

Results

We recently demonstrated that complete targeted deletion of the *Vglut2* gene in the mouse results in immediate neonatal death (Wallén-Mackenzie et al., 2006). To establish that the phenotype was attributable to a nervous system-specific defect, we crossbred our mice carrying the conditionally targeted *Vglut2* allele to the *nestin*-cre mouse line (Tronche et al., 1999). The nervous system-specific removal of VGLUT2 phenocopied the complete deletion, confirming that specific deletion in the nervous system is sufficient to cause lethal defects. This experiment also verified that removal of the *Vglut2* conditional targeted allele was possible in a tissue-specific manner (data not shown). *Vglut2* expression starts early during development and *Vglut2* mRNA can be readily detected in several brain structures (e.g., the developing cortex, hypothalamus, thalamus, tegmentum, and medulla already at embryonic day 12.5) (Wallén-Mackenzie et al., 2006). We used mice expressing the Cre protein under regulation of the CaMKIIα promoter to eliminate *Vglut2* in higher brain regions at later stages and to avoid the early lethality resulting from germ line deletion of *Vglut2*. CaMKIIα-Cre mice express Cre from postnatal day 15 (P15) and onward in the hippocampus, cortex, and amygdala (Minichiello et al., 1999). We confirmed the described expression pattern of the CaMKIIα-Cre mice by crossing them with two different reporter mice. Offspring from crossing with Z/AP reporter mice (Lobe et al., 1999) were analyzed at P6 by staining of brain sections for lacZ and alkaline phosphatase activity, which demonstrated a lack of Cre activity at this stage (supplemental Fig. 1, available at www.jneurosci.org as supplemental material). In addition, offspring from crossing with Tau^{mGFP} reporter mice were analyzed at P21 by staining of brain sections for LacZ activity, which showed expected expression in hippocampus, cortex, and amygdala (Hippenmeyer et al., 2005) (supplemental Fig. 1, available at www.jneurosci.org as supplemental material).

Specific deletion of *Vglut2* in discrete regions of the cortex, hippocampus, and amygdala

CaMKIIα-Cre mice were bred with mice carrying the conditional allele of *Vglut2* to generate *Vglut2*$^{f/f;CaMKII\text{-}Cre}$ mice (Fig. 1*A*). Mice homozygous for the conditional allele and carrying the Cre allele ($n = 52$) were born in normal Mendelian ratios and were viable to adulthood. We determined the efficiency of the deletion in the *Vglut2*$^{f/f;CaMKII\text{-}Cre}$ mutant mice using *in situ* hybridization with a probe recognizing the 3′ end of *Vglut2* mRNA. A restricted number of neuronal populations in two areas, the cortex and amygdala, could be identified that had lost their expression of *Vglut2* mRNA. The cortical retrosplenial group (RSG), the hippocampal subiculum and presubiculum, as well as some neurons scattered in the entorhinal and piriform cortex and in cortical layers III and V/VI composed the cortical area (Fig. 1; supplemental Fig. 2, available at www.jneurosci.org as supplemental material). Four amygdaloid nuclei, the anterior cortical (ACo), the posterolateral cortical (PLCo), the basomedial amygdaloid (BMA), the medial amygdaloid (MeA) nuclei together with the bed nucleus of the accessory olfactory tract (BAOT) composed the amygdaloid area (Fig. 1; supplemental Fig. 2, available at www.jneurosci.org as supplemental material). Slightly reduced levels of *Vglut2* mRNA could be detected by *in situ* hybridization in the thalamus/hypothalamus area of one animal; however, this was not observed in analyses of additional animals. Instead, a more detailed analysis of the thalamus showed that *Vglut2* mRNA is not lacking from any of the investigated thalamic subnuclei and that the levels of expression appeared similar in *Vglut2*$^{f/f;CaMKII\text{-}Cre}$ mutant mice and littermate controls (supplemental Fig. 3, available at www.jneurosci.org as supplemental material). We did not observe any major changes in any of the other brain regions in which *Vglut2* is normally expressed, including the inferior and superior colliculus, lateral parabrachial nucleus, pontine reticular nuclei, periaqueductal gray, parabigeminal, red, mammilary, subthalamic, and geniculate nuclei (supplemental Fig. 2, available at www.jneurosci.org as supplemental material). In conclusion, *Vglut2* expression was selectively deleted in CaMKIIα-expressing areas.

Loss of VGLUT2 presynaptic labeling in projection areas

The loss of *Vglut2* mRNA leads to the subsequent loss of VGLUT2 protein production. Our previous results from electron microscopy studies have demonstrated that loss of VGLUT2 results in malformed and reduced number of presynaptic vesicles (Wallén-Mackenzie et al., 2006). By using a VGLUT2-specific antibody, we analyzed whether changes in VGLUT2 protein levels were detectable in the presynaptic terminals of the projection target areas of the neurons that had lost *Vglut2* mRNA expression. The striatum, cortex, and hippocampus all receive glutamatergic in-

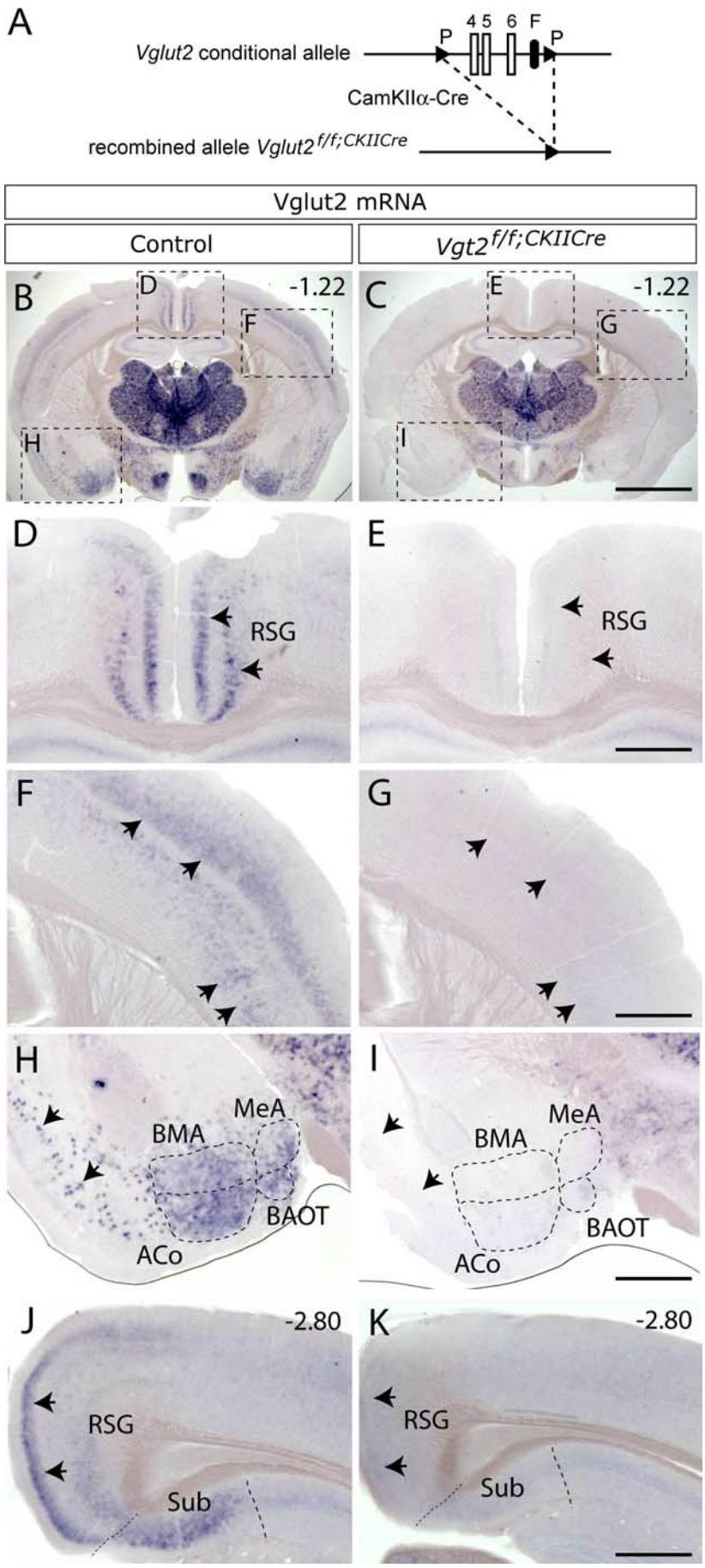

put from the affected areas. In the striatum, nucleus accumbens, and cortex of *Vglut2*$^{f/f;CaMKII\text{-}Cre}$ mice, a significant reduction in VGLUT2-immunopositive varicosities was detected (30%, $p = 0.0006$; 11%, 1×10^{-6}; and 16%, 0.006, respectively) (Fig. 2*A–H*,*Q*,*R*) (data not shown). Also, in the dentate gyrus of the *Vglut2*$^{f/f;CaMKII\text{-}Cre}$ mouse hippocampus, a readily detectable and significant reduction of VGLUT2-immunopositive varicosities was detected (32%; $p = 0.036$) (Fig. 2*I–L*,*S*). The cerebellar granular layer, which does not receive projections from the affected areas, was used as a control area and no differences in the number of VGLUT2-immunopositive varicosities could be detected in this region (Fig. 2*M–P*,*T*). These data show that loss of *Vglut2* mRNA leads to a significant reduction of VGLUT2-positive varicosities in the striatum, nucleus accumbens, cortex, and hippocampus. The detected loss of VGLUT2 in the dentate gyrus prompted us to test synaptic function in the glutamatergic synapses in the molecular layer of the dentate gyrus by electrophysiological measurements. However, no obvious indication of a disrupted synaptic transmission was observed when comparing basal synaptic strength, short-term plasticity, and long-term potentiation in the hippocampus between *Vglut2*$^{f/f;CaMKII\text{-}Cre}$ and control mice (supplemental Fig. 4, available at www.jneurosci.org as supplemental material). Furthermore, we also examined the basic properties of glutamatergic synaptic transmission in the striatum by performing extracellular recordings in acute corticostriatal brain slices, but no difference between control and *Vglut2*$^{f/f;CaMKII\text{-}Cre}$ animals was detected

←

Figure 1. Targeted deletion of *Vglut2* from higher brain regions. ***A***, Scheme of recombination event in mice carrying the *Vglut2* conditional allele. The loxP (P) flanked *Vglut2* exons 4, 5, and 6 have been excised by breeding to transgenic mice carrying CaMKIIα-Cre generating *Vglut2*$^{f/f;CaMKII\text{-}Cre}$ mice. ***B–I***, *Vglut2 in situ* hybridization on coronal brain sections from 8-week-old adult *Vglut2*$^{f/f;CaMKII\text{-}Cre}$ and littermate control mice. As opposed to control mice (***B***), cells expressing *Vglut2* mRNA were not detectable in specific areas of the cortex, amygdala, and hippocampus in *Vglut2*$^{f/f;CaMKII\text{-}Cre}$ mice (***C***). ***D–I***, Close-ups as indicated in ***B*** and ***C***, which demonstrate that cells expressing *Vglut2* mRNA were absent in the RSG of the medial cortex (***D***, ***E***, arrows) and in cortical layers III and V/VI (***F***, ***G***, arrows) in *Vglut2*$^{f/f;CaMKII\text{-}Cre}$ mice. *Vglut2* mRNA-expressing cells were also absent in the ACo, BAOT, BMA, and MeA nuclei as well as in piriform cortex (***H***, ***I***, arrows). ***J***, ***K***, *Vglut2* mRNA-positive cells were present in the subiculum (Sub) in littermate control mice (***J***) but not in *Vglut2*$^{f/f;CaMKII\text{-}Cre}$ mice (***K***). Scale bars: ***B***, ***C***, 1.8 mm; ***D–I***, 0.55 mm. Bregma levels are shown in the top right corner.

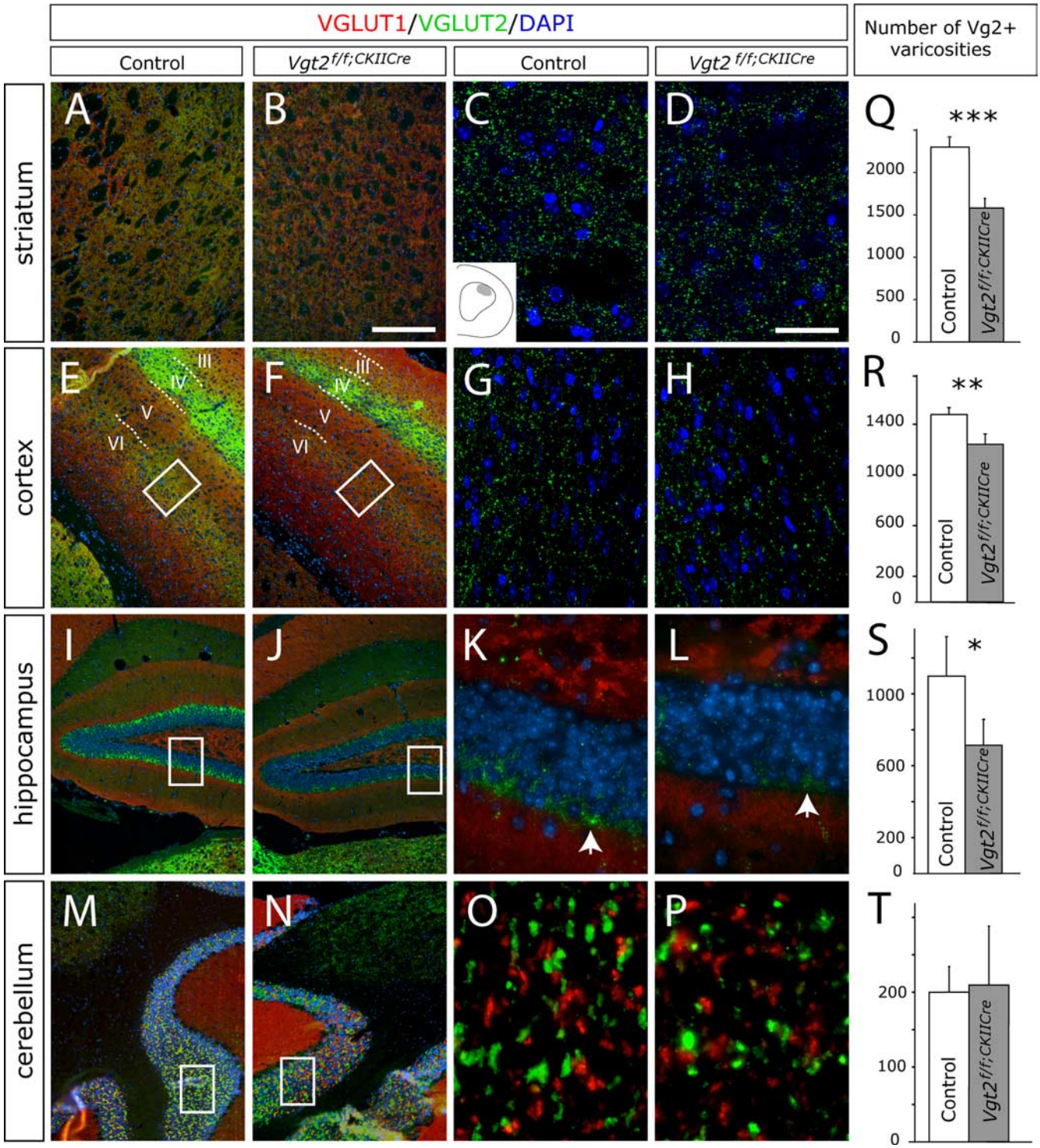

Figure 2. *Vglut2*$^{f/f;CaMKII\text{-}Cre}$ mice have reduced numbers of VGLUT2-positive varicosities in the striatum, cortex, and hippocampus. ***A–P***, VGLUT1 (red) and VGLUT2 (green) immunofluorescence and DAPI nuclear stain (blue) on brain sections from adult animals. In the striatum (***A–D***), cortex (***E–H***), and hippocampus (***I–L***), the number of VGLUT2-immunopositive varicosities appeared reduced in the *Vglut2*$^{f/f;CaMKII\text{-}Cre}$ mice compared with control, whereas the number of terminals in the cerebellum appeared normal (***M–P***). To improve clarity, the red channel representing VGLUT1-positive stain, which is shown in low-magnification pictures (***A***, ***B***, ***E***, ***F***, ***I***, ***J***, ***M***, ***N***) is not shown in high-magnification pictures (***C***, ***D***, ***G***, ***H***, ***K***, ***L***, ***O***, ***P***). The analyzed area of the dorsolateral striatum is shown in the schematic inset in ***C***, of the cortical layers V/VI is indicated by roman numerals and boxed in ***E*** and ***F***, and of the dentate gyrus is boxed in ***I*** and ***J***. Scale bars: ***A***, ***B***, ***E***, ***F***, ***I***, ***J***, ***M***, ***N***, 130 μm; ***C***, ***D***, ***G***, ***H***, ***K***, ***L***, ***O***, ***P***, 22 μm. ***Q–T***, Quantification of VGLUT2-immunopositive varicosities using Volocity software demonstrated a significant reduction in the striatum with 30% ($p = 0.0006$), cortex with 16% ($p = 0.006$), and dentate gyrus of the hippocampus with 32% ($p = 0.036$) in the *Vglut2*$^{f/f;CaMKII\text{-}Cre}$ mice compared with controls. No change in the cerebellum was seen. Error bars indicate SEM; $^{*}p < 0.05$, $^{**}p < 0.01$, $^{***}p < 0.001$ compared with control littermates.

in response to increased stimulation intensity or pulse number in 10 or 25 Hz (supplemental Fig. 5, available at www.jneurosci.org as supplemental material). Thus, the detected 30% loss of VGLUT2 striatal terminals may not result in a measurable difference by these methods. In addition, the high abundance of VGLUT1-positive terminals in the striatum could possibly mask effects originating from loss of VGLUT2.

Increased activity and risk taking in *Vglut2*$^{f/f;CaMKII\text{-}Cre}$ mice

The normal development and life span of *Vglut2*$^{f/f;CaMKII\text{-}Cre}$ mice allowed us to determine whether lost VGLUT2-mediated neurotransmission affected behavior. For the behavioral analyses, mice older than 8 weeks were used to ensure that the *Vglut2* deletion mediated by CaMKIIα-Cre was complete. In the elevated plus maze (Pellow et al., 1985), *Vglut2*$^{f/f;CaMKII\text{-}Cre}$ mice spent significantly less time in the closed arm but instead more time in the outer open arm compared with controls (110%; $p = 0.022$) (Fig. 3*A*). They also entered all areas more frequently than control mice (Fig. 3*B*) and had a higher general activity (148%; $p = 0.0002$) relative to controls. To further explore the reduced anxiety and increased activity displayed by the mice in the plus maze, we turned to the more sensitive MCSF test (Meyerson et al., 2006). In the MCSF test, the mouse is exposed to various challenges for the assessment of general activity, exploration, risk assessment, risk-taking, and shelter-seeking behavior. Again, as can be seen in supplemental Table 1 (available at www.jneurosci.org as supplemental material), the *Vglut2*$^{f/f;CaMKII\text{-}Cre}$ mice displayed a significant increase (40%; $p = 0.0008$) in their total activity. Also, the *Vglut2*$^{f/f;CaMKII\text{-}Cre}$ mice remained active during the entire test trial and were significantly more active relative to the control mice during the last three 5 min periods of the total 20 min trial time (Fig. 3*C*). Furthermore, the *Vglut2*$^{f/f;CaMKII\text{-}Cre}$ mice made more visits (43%; $p = 0.0006$) and had a shorter duration per visit (40%; $p = 0.0005$) in the corridors, which indicate that the *Vglut2*$^{f/f;CaMKII\text{-}Cre}$ mice switched zones more often than the controls.

The MCSF was also used to measure additional behaviors. *Vglut2*$^{f/f;CaMKII\text{-}Cre}$ mice made significantly more visits to the hurdle than the controls, indicating an increased exploratory activity (55%; $p = 0.005$). Measures of risk assessment (parameters related to the slope) revealed differences between the two groups. *Vglut2*$^{f/f;CaMKII\text{-}Cre}$ mice made more visits to the slope (Fig. 3*D*) and had a shorter duration per visit to the slope (40%; $p = 0.015$), indicating a higher risk assessment behavior relative to the control mice. Measures of risk-taking behavior (parameters related to the bridge and the central circle) showed that *Vglut2*$^{f/f;CaMKII\text{-}Cre}$ mice made more visits both to the bridge (27%; $p = 0.038$) and the central circle (80%; $p = 0.0022$) (Fig. 3*E*) and had a longer duration in the central circle (75%; $p = 0.0059$) than control animals. Furthermore, measures of shelter-seeking behavior (parameters related to the dark corner room) showed that the *Vglut2*$^{f/f;CaMKII\text{-}Cre}$ mice had a shorter duration (52%; $p = 0.0002$) and duration per visit (Fig. 3*F*) in the dark corner room, indicating less shelter seeking than the controls. The emotional state of the mice was further analyzed by the forced-swim test, which is a commonly used model for depression (Porsolt et al., 1977). However, no significant differences between *Vglut2*$^{f/f;CaMKII\text{-}Cre}$ and control mice were observed.

Together, these data suggest that *Vglut2*$^{f/f;CaMKII\text{-}Cre}$ mice are hyperactive and are characterized by less avoidance of open areas, less shelter seeking and abnormal risk behavior, which may indicate a lower emotional reactivity than in the control animals.

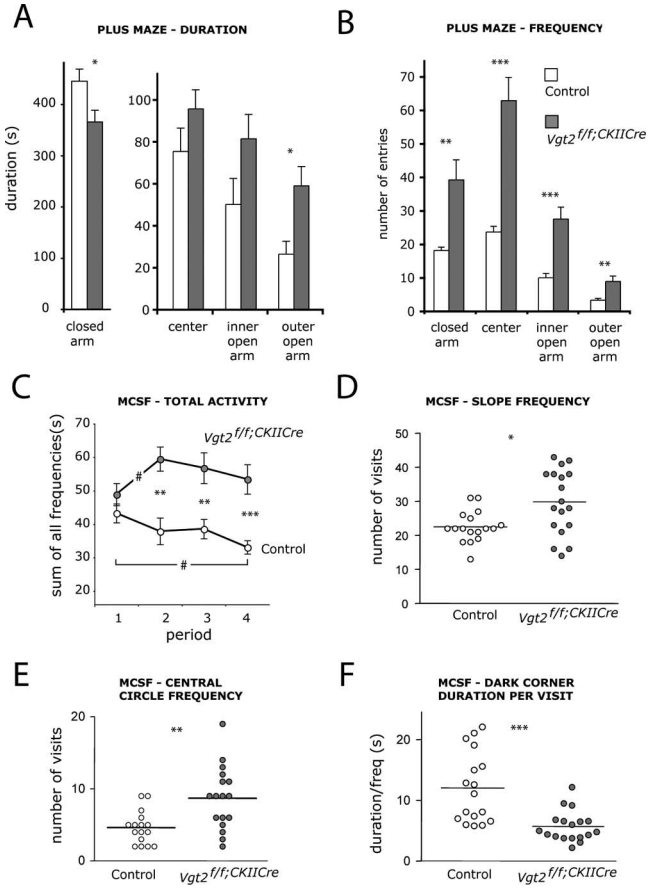

Figure 3. *Vglut2*$^{f/f;CaMKII\text{-}Cre}$ mice are hyperactive and display reduced anxiety-like behavior. ***A***, ***B***, Elevated plus maze analysis on adult *Vglut2*$^{f/f;CaMKII\text{-}Cre}$ mice and control littermates. *Vglut2*$^{f/f;CaMKII\text{-}Cre}$ mice spend significantly more time ($p = 0.022$) on the outer open arm and less time in the closed arm ($p = 0.038$), suggesting reduced anxiety-like behavior in *Vglut2*$^{f/f;CaMKII\text{-}Cre}$ mice ($n = 10$/group) (***A***). The number of entries in all four different areas of the plus maze is significantly higher for *Vglut2*$^{f/f;CaMKII\text{-}Cre}$ mice compared with controls (closed arm, $p = 0.0002$; center, $p = 0.0002$; inner open arm, $p = 0.0015$; outer open arm, $p = 0.010$), suggesting hyperactivity (***B***). ***C–F***, MCSF analysis on adult *Vglut2*$^{f/f;CaMKII\text{-}Cre}$ mice and control littermates. The sum of visits to all zones in the MCSF analysis split into four 5 min periods show that the activity in *Vglut2*$^{f/f;CaMKII\text{-}Cre}$ mice increase between the first and second 5 min period ($p = 0.019$). In control littermates, the activity is significantly lower in period 4 ($p = 0.0097$) than in period 1 and shows a tendency to decrease over time. In *Vglut2*$^{f/f;CaMKII\text{-}Cre}$ mice, the activity is higher in period 4 than in period 1, suggesting that the mutant mice have difficulties in adapting to new environments. Furthermore, during periods 2–4, the *Vglut2*$^{f/f;CaMKII\text{-}Cre}$ mice had a significantly higher activity ($p = 0.0011$, $p = 0.0035$, $p = 0.0002$, respectively) compared with the control littermates ($n = 16–18$/group) (***C***). The number of visits to the slope is significantly increased ($p = 0.0153$) in *Vglut2*$^{f/f;CaMKII\text{-}Cre}$ mice compared with controls, indicating altered risk assessment behavior (***D***). *Vglut2*$^{f/f;CaMKII\text{-}Cre}$ mice make significantly more visits to the central circle compared with littermate controls ($p = 0.0022$), indicating less avoidance of open areas (***E***). The duration of each visit to the dark corner room is significantly shorter ($p = 0.0002$) in *Vglut2*$^{f/f;CaMKII\text{-}Cre}$ mice compared with controls ($n = 16–18$/group) (***F***). $^{*}p < 0.05$, $^{**}p < 0.01$, $^{***}p < 0.001$ compared with control littermates (***C–F***) (Mann–Whitney *U* test); $^{\#}p < 0.05$ compared with the respective period 1 (Wilcoxon signed-rank test). Error bars indicate SEM.

Social and cognitive deficits in *Vglut2*$^{f/f;CaMKII\text{-}Cre}$ mice

Hyperactive behavior has been associated to the positive symptoms of schizophrenia, whereas blunted emotional expression has been associated to the negative symptoms (Ellenbroek et al., 2000). To get a wider assessment of a potential resemblance of the behavior of the *Vglut2*$^{f/f;CaMKII\text{-}Cre}$ mice to schizophrenia-like behaviors, analyses of relevance for negative as well as cognitive dysfunctions were performed (Swerdlow and Geyer, 1998; Ellenbroek et al., 2000; Arguello and Gogos, 2006). Negative symptoms include impaired social behavior, and therefore, we tested the *Vglut2*$^{f/f;CaMKII\text{-}Cre}$ mice for this parameter. The social dominance tube test revealed that *Vglut2*$^{f/f;CaMKII\text{-}Cre}$ mice were characterized by significantly fewer wins, which could suggest a less dominant phenotype (Fig. 4*A*). We also tested the mice twice in a social interaction test. *Vglut2*$^{f/f;CaMKII\text{-}Cre}$ mice spent significantly more time than controls interacting with a newly introduced

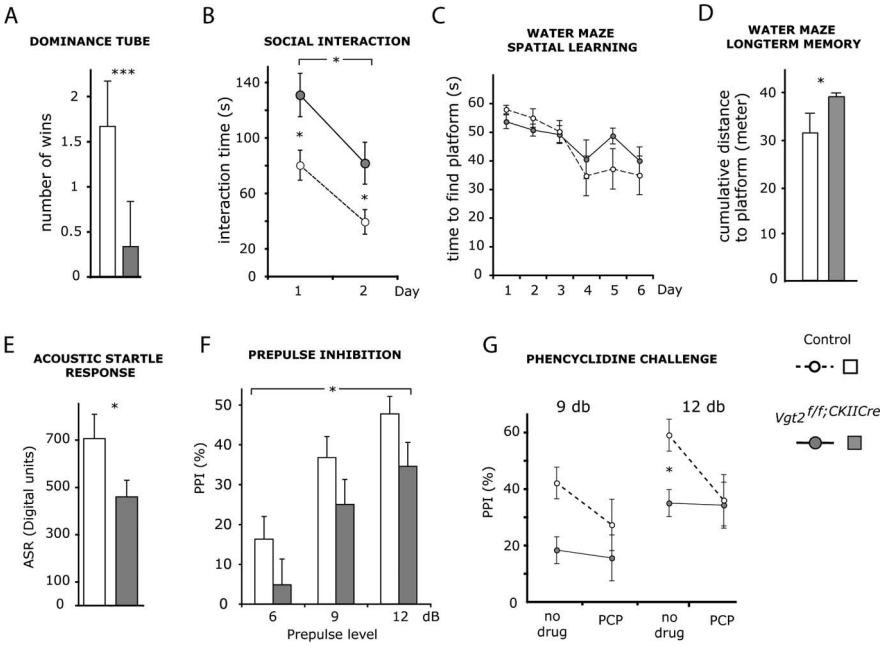

Figure 4. Social deficits, impaired long-term memory, and pharmacologically reversible sensory filtering deficits in *Vglut2*$^{f/f;CaMKII\text{-}Cre}$ mice. ***A***, ***B***, Social behavior analysis on adult *Vglut2*$^{f/f;CaMKII\text{-}Cre}$ mice and control littermates. The number of wins in the social dominance tube test show that *Vglut2*$^{f/f;CaMKII\text{-}Cre}$ mice (filled bar; $n = 9$) display a less dominant phenotype than controls (open bar; $n = 9$; $p = 0{,}00004$) (***A***). The total time spent in interaction during two 10 min social interaction sessions separated by 48 h show that *Vglut2*$^{f/f;CaMKII\text{-}Cre}$ mice (filled circles; $n = 8$) spend significantly more time in interaction than controls (open circles; $n = 8$) across test sessions ($p = 0.014$; two-way repeated-measures ANOVA, effect of genotype). Both genotypes showed a comparable decrease in interaction time during the second session as a result of adaptation to the test situation ($p = 0.0001$; two-way repeated-measures ANOVA, effect of day) (***B***). ***C***, ***D***, Learning and memory analysis in the Morris water maze. Spatial learning displayed as mean time (5 consecutive swims) to find platform over 6 acquisition days. Both *Vglut2*$^{f/f;CaMKII\text{-}Cre}$ mice (filled circles; $n = 9$) and controls (open circles; $n = 5$) showed significant learning across the acquisition days ($p < 0.0001$; two-way repeated-measures ANOVA, effect of day) (***C***). Long-term spatial memory measured as cumulative distance to previous platform position 48 h after the last day of acquisition is shown. *Vglut2*$^{f/f;CaMKII\text{-}Cre}$ mice (filled circles; $n = 9$) showed significantly impaired spatial long-term memory ($p = 0.0058$; one-way ANOVA, effect of genotype) when compared with controls (open circles; $n = 5$) (***D***). ***E–G***, Acoustic startle response (ASR) and prepulse inhibition analyses. *Vglut2*$^{f/f;CaMKII\text{-}Cre}$ mice (filled bar; $n = 22$) had significantly lower ASR ($p = 0.029$; one-way ANOVA, effect of genotype) than their control littermates (open bar; $n = 21$) (***E***). Prepulse inhibition of the acoustic startle at three prepulse intensities show that *Vglut2*$^{f/f;CaMKII\text{-}Cre}$ mice (filled bars; $n = 22$) displayed a significantly lower overall prepulse inhibition than control littermates (open bars; $n = 21$) ($p = 0.025$; three-way repeated-measures ANOVA, effect of genotype) (***F***). Prepulse inhibition before and after challenge with PCP at prepulse intensities of 9 and 12 dB show that a significant difference between *Vglut2*$^{f/f;CaMKII\text{-}Cre}$ mice (filled circles; $n = 4$) and their control littermates (open circles; $n = 5$) was observed at the 12 dB intensity before but not after PCP treatment ($p = 0.037$, Student's *t* test). Error bars indicate SEM; $^{*}p < 0.05$, $^{***}p < 0.001$ compared with control littermates.

counterpart across both days in a 2 d trial (Fig. 4*B*). This increase in interaction time was not explained by their general increase in motility, because the total number of interactions did not differ between *Vglut2*$^{f/f;CaMKII\text{-}Cre}$ mice and controls (data not shown). Both *Vglut2*$^{f/f;CaMKII\text{-}Cre}$ mice and controls learned equally fast to recognize their counterpart as evidenced by a comparable decrease in interaction time on the second day (Fig. 4*B*). To investigate cognitive abilities, animals were tested for spatial learning and long-term memory in a modified Morris water maze test. Both *Vglut2*$^{f/f;CaMKII\text{-}Cre}$ mice and controls showed significant learning over the 6 acquisition days (Fig. 4*C*). Although there was no significant effect of genotype on learning, *Vglut2*$^{f/f;CaMKII\text{-}Cre}$ mice displayed significantly impaired spatial long-term memory compared with controls (Fig. 4*D*). The data were also analyzed with regard to time spent in the target quadrant during the test day, demonstrating a tendency for *Vglut2*$^{f/f;CaMKII\text{-}Cre}$ mice ($n = 8$; 25.3 ± 2.3) to spend less time in the target quadrant compared with controls ($n = 5$; 31.2 ± 5.9). This test demonstrated that learning abilities were similar between *Vglut2*$^{f/f;CaMKII\text{-}Cre}$ mice and controls, whereas long-term memory of *Vglu2*$^{f/f;CaMKII\text{-}Cre}$ mice was significantly impaired.

To assess the integrity of the preattentive filter mechanisms that are commonly disturbed in schizophrenia-like behavior, we measured prepulse inhibition (PPI) of the acoustic startle response in *Vglut2*$^{f/f;CaMKII\text{-}Cre}$ mice and controls. The PPI paradigm allows for the study of a homologous behavior across species and is therefore well suited for investigating information processing in both rodents and humans (Swerdlow and Geyer, 1998; Arguello and Gogos, 2006). Interestingly, *Vglut2*$^{f/f;CaMKII\text{-}Cre}$ mice showed a significantly impaired PPI across all tested prepulse intensities, 6, 9, and 12 dB, when compared with controls (Fig. 4*F*), and also showed a lower acoustic startle response (Fig. 4*E*). A subgroup of mice were tested for PPI, challenged with the glutamate antagonist phencyclidine 48 h later, and then retested to investigate glutamate system integrity. No interaction effect could be demonstrated in this group of animals, when analyzing treatment by genotype. However, when *Vglut2*$^{f/f;CaMKII\text{-}Cre}$ mice and controls were tested at the 12 dB intensity before phencyclidine treatment, they differed significantly in their PPI levels (Fig. 4*G*). The difference did not remain after treatment, tentatively suggesting that *Vglut2*$^{f/f;CaMKII\text{-}Cre}$ mice were less susceptible to the disruptive effects of phencyclidine on PPI at this prepulse intensity.

No effect on distribution of neuronal populations by the *Vglut2* deletion

Given the substantial alteration in the *Vglut2*$^{f/f;CaMKII\text{-}Cre}$ mice in higher brain functions such as cognitive, social, and emotional behavior as a result of the selective *Vglut2* deletion, we wanted to investigate the putative effects on additional neuronal populations. First, real-time PCR was used to quantify the amounts of all three vesicular glutamate transporters, including *Vglut3*, which is not exclusively expressed in glutamatergic neurons (Gras et al., 2002), and the excitatory amino acid carrier 1 (*EAAC1*) in mRNA extracted from four different regions of the brain in which *Vglut2* mRNA and/or VGLUT2-positive presynaptic terminals had been lost, the amygdala, cortex, hippocampus, and striatum (Figs. 1, 2). mRNA extracted from the cerebellum was used as control region because it was not affected by the *Vglut2* mutation. As expected, based on *in situ* data (Fig. 1), our results demonstrated that *Vglut2* mRNA levels were significantly decreased in the hippocampus and cortex. *Vglut1* and *EAAC1* mRNA levels were not significantly affected in any of the brain regions analyzed; however, we could detect a small but significant decrease of *Vglut3* in the cortex (Fig. 5*A*). To detect possible changes in neuronal distribution and density, brain sections were analyzed using *in situ* hybridization. No major changes of *Vglut1*-expressing glutamatergic neurons in the cortex and hippocampus (Fig. 5*B–E*) could be detected. Inhibitory neuronal populations,

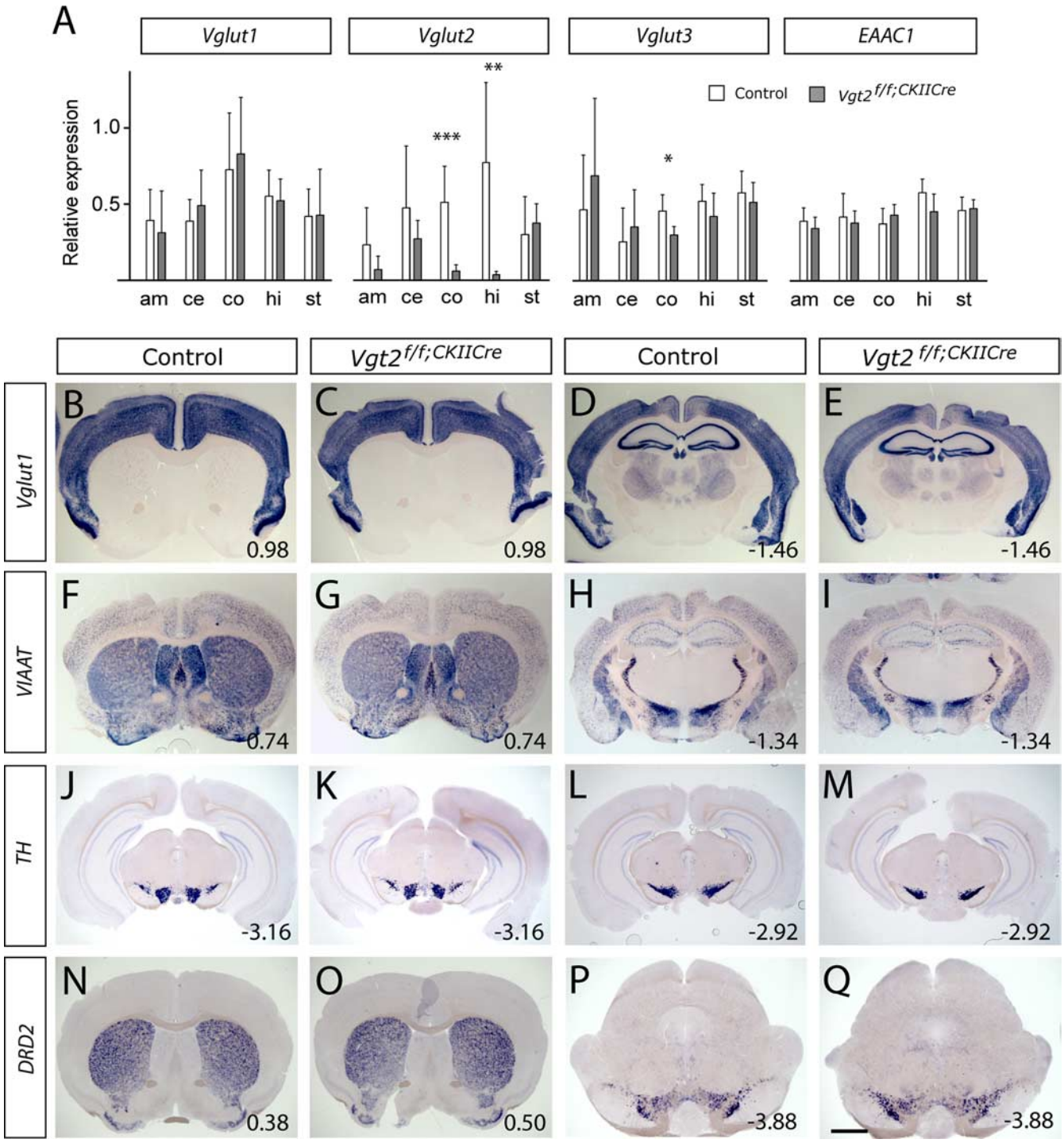

Figure 5. Distribution and levels of *Vglut1*, *VIAAT*, *TH*, and *DRD2* mRNA appear unaffected in *Vglut2*$^{f/f;CaMKII\text{-}Cre}$ mice. ***A***, Quantitative real-time PCR was used to measure mRNA levels of *Vglut1*, *Vglut2*, *Vglut3*, and excitatory amino acid transporter 1 (*EAAC1*) in the amygdala (am), cerebellum (ce), cortex (co), hippocampus (hi), and striatum (st). A significant decrease was found in *Vglut2* mRNA in cortex ($p = 0.0004$) and hippocampus ($p = 0.0012$) of *Vglut2*$^{f/f;CaMKII\text{-}Cre}$ mice, as well as for *Vglut3* mRNA in cortex of *Vglut2*$^{f/f;CaMKII\text{-}Cre}$ mice ($p = 0.014$). The relative expressions only enable direct comparison between control and *Vglut2*$^{f/f;CaMKII\text{-}Cre}$ mice within each transcript type. The white bars represent control mice ($n = 7$), and the gray bars represent *Vglut2*$^{f/f;CaMKII\text{-}Cre}$ mice ($n = 6$). Error bars indicate SEM; $^*p < 0.05$, $^{**}p < 0.01$, $^{***}p < 0.001$ compared with control littermates. ***B–Q***, *In situ* hybridization on brain sections demonstrated similar distributions of *Vglut1*, *VIAAT*, *TH*, and *D2DR* mRNA in adult control and *Vglut2*$^{f/f;CaMKII\text{-}Cre}$ mouse brains. The sections show *Vglut1* in the cortex and hippocampus (***B–E***); *VIAAT* in the cortex, striatum, and nucleus accumbens (***F***, ***G***) and in the hippocampus, zona incerta, subincertal nucleus, the reticular thalamic nuclei, and the central and medial amygdaloid nuclei (***H***, ***I***); *TH* in the ventral tegmental area (***J***, ***K***) and the substantia nigra (***L***, ***M***); and *DRD2* in the striatum, olfactory tubercle, and nucleus accumbens (***N***, ***O***) and in the ventral tegmental area (***P***, ***Q***). Scale bar, 0.9–1.3 mm. Bregma levels are shown in the bottom right corner.

as detected by their expression of vesicular inhibitory amino acid transporter (*VIAAT*), appeared normal in all areas analyzed (Fig. 5*F–I*).

The described reciprocal action of glutamate and dopamine in cortical and subcortical regions warranted special attention to be drawn to the midbrain dopamine neurons. Components of the nigrostriatal and mesocorticolimbic systems were detected by their expression of tyrosine hydroxylase (*TH*) (Fig. 5*J–M*) (data

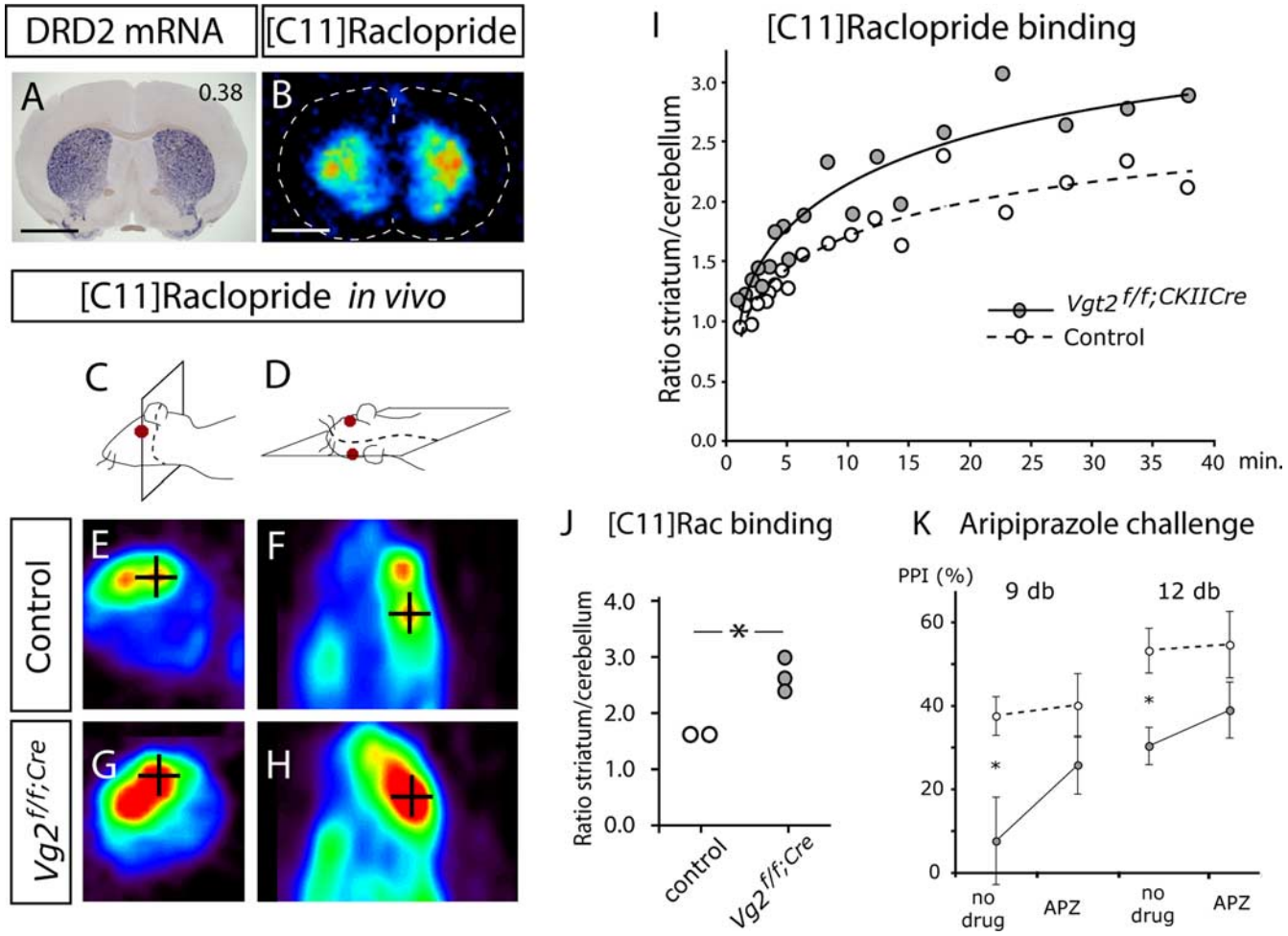

Figure 6. Increased number of D2DR *in vivo* binding sites in the striatum of *Vglut2*$^{f/f;CaMKII\text{-}Cre}$ mice. ***A***, *In situ* hybridization showing the distribution of cells positive for DRD2 mRNA in the striatum (blue). Scale bar, 1.85 mm. Bregma level of 0.38 is indicated in the top right corner. ***B***, [^{11}C]Raclopride binding to brain section *in vitro*. The highest binding was detected in the area of the striatum (outline of brain section is indicated with a stippled line). ***C–H***, PET scans showing retention of [^{11}C]raclopride in striatum (black cross defines a three-dimensional point). Coronal (***C***, ***E***, ***G***) and sagittal (***D***, ***F***, ***H***) views are shown. In the sagittal view, head glands can be seen rostrolaterally of the striatum. This glandular retention of radioactivity is observed with many PET tracers and is not attributable to specific binding to receptors. ***I***, [^{11}C]Raclopride uptake curves shown as the ratio between striatum and cerebellum measured in two animals of each genotype. *Vglut2*$^{f/f;CaMKII\text{-}Cre}$ mice tend to have a progressively higher binding ratio over a 40 min period. ***J***, [^{11}C]Raclopride uptake after 40 min shown as the ratio between striatum and cerebellum. Female *Vglut2*$^{f/f;CaMKII\text{-}Cre}$ mice have a significantly higher binding ratio (1.7-fold) than control females ($n = 2$–3/group; $p = 0.031$). ***K***, Prepulse inhibition before and after challenge with aripiprazole at prepulse intensities of 9 and 12 dB above background. A significant difference in prepulse inhibition between *Vglut2*$^{f/f;CaMKII\text{-}Cre}$ mice (filled circles; $n = 11$) and controls (open circles; $n = 11$) was observed before but not after aripiprazole treatment (9 dB, $p = 0.017$; 12 dB, $p = 0.0039$, Student's *t* test). Error bars indicate SEM; *$p < 0.05$ compared with control littermates.

not shown) and the dopamine D_2 receptor (*DRD2*) (Fig. 5*N–Q*). The distribution and density of dopaminergic neurons in the substantia nigra pars compacta (Fig. 5*J–M*, *P*, *Q*) and ventral tegmental area were normal (Fig. 5*J*, *K*, *P*, *Q*) as were the *DRD2*-expressing neurons in the striatum (Fig. 5*N*, *O*). Additional target areas of the mesolimbocortical pathway, including the nucleus accumbens and the olfactory tubercle were also assayed for *DRD2* expression, and no difference was found between *Vglut2*$^{f/f;CaMKII\text{-}Cre}$ and control brains. In summary, the data demonstrate that the cellular distribution and density of *Vglut1*-expressing glutamatergic neurons, *VIAAT*-expressing inhibitory neurons, midbrain dopaminergic neurons, and their target neurons, as detected by mRNA expression, remain similar in the controls and *Vglut2*$^{f/f;CaMKII\text{-}Cre}$ mutants.

Dopamine receptor upregulation and normalization of PPI

We were interested in examining putative effects on the dopaminergic system further. DRD2 distribution was analyzed in frozen brain sections by autoradiography after binding of the radiolabeled DRD2 ligand [^{11}C]raclopride. In accordance with the striatal expression of DRD2 (Fig. 6*A*), a strong specific binding of [^{11}C]raclopride was localized to the striatum (Fig. 6*B*). Comparison of *Vglut2*$^{f/f;CaMKII\text{-}Cre}$ and control mice did not reveal a difference in [^{11}C]raclopride-specific binding on striatal sections (control, 0.63 ± 0.08 AU; *Vglut2*$^{f/f;CaMKII\text{-}Cre}$, 0.71 ± 0.08 AU; $n = 6$; $p = 0.15$).

We next used positron emission tomography (PET) to measure binding of [^{11}C]raclopride in living mice (Fig. 6*C–H*, red area). In the PET scans, an intense signal was detected in the area of the striatum, nucleus accumbens, and the olfactory tubercle (hereafter shortened the striatal area). The cerebellum was devoid of any significant binding and the kinetics of radioactivity in the cerebellum was similar in all animals (data not shown). To normalize for body weight and administered radioactivity, the ratio between uptake in the striatal area and cerebellum was calculated. A progressively higher degree of [^{11}C]raclopride binding was observed in the striatal area of *Vglut2*$^{f/f;CaMKII\text{-}Cre}$ mice compared with control mice (Fig. 6*I*). In measurements performed 40 min

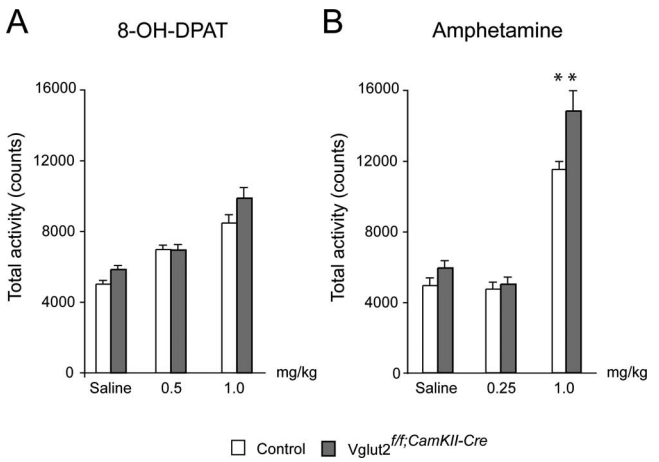

Figure 7. Increased sensitivity for amphetamine in *Vglut2*$^{f/f;CaMKII\text{-}Cre}$ mice. Vglut2$^{f/f;CaMKII\text{-}Cre}$ and control mice were treated with a low or a high dose of amphetamine or 8-OH-DPAT ($n = 8$ for both genotypes and treatments). Saline injections were used as controls for methodological background. After treatment, total activity was recorded in a fully automated motor activity cage during 1 h, in which each movement was registered as one count. ***A***, Administration of 8-OH-DPAT did not result in any detectable differences between the two groups. ***B***, On the contrary, administration of amphetamine (1 mg/kg) increased the activity of Vglut2$^{f/f;CaMKII\text{-}Cre}$ animals ($p < 0.01$) to a larger extent compared with control animals. This result supports the suggestion that the dopaminergic neurons are altered downstream of Vglut2-mediated neurotransmission in Vglut2$^{f/f;CaMKII\text{-}Cre}$ mice, and that this alteration may be a partial reason for their changed behavior. Error bars indicate SEM; $^{**}p < 0.01$.

after injection, there was a significant 70% increase ($p = 0.031$) of [^{11}C]raclopride binding in the striatum of*Vglut2*$^{f/f;CaMKII\text{-}Cre}$ mice (Fig. 6*J*). These experiments suggest an effect of the *Vglut2* targeted mutation on the activity of the dopamine system, a finding that was further corroborated by electrochemical detection of dopamine in striata of of*Vglut2*$^{f/f;CaMKII\text{-}Cre}$ and control mice using HPLC. Analysis of homogenates from freshly prepared tissue showed a significant 17% upregulation of dopamine content in the mutant striatum (control, 0.019 ± 0.001; *Vglut2*$^{f/f;CaMKII\text{-}Cre}$, 0.023 ± 0.001 fmol/g wet tissue; $n = 20$; $p = 0.04$). Subsequently, we analyzed the behavior of the mice in response to drugs that affect the dopamine system. First, the novel dopamine-stabilizing antipsychotic drug aripiprazole was tested for its ability to attenuate the impaired PPI demonstrated in *Vglut2*$^{f/f;CaMKII\text{-}Cre}$ mice (Fig. 6*K*). In similarity to the phencyclidine experiment (Fig. 4*G*), no significant genotype by treatment interaction effect could be shown in this group of animals. Nevertheless, whereas *Vglut2*$^{f/f;CaMKII\text{-}Cre}$ mice and controls displayed significantly different PPI levels at the 9 and 12 dB intensities, this difference was absent after aripiprazole treatment (Fig. 6*K*). This suggests a trend toward a normalization of PPI in aripiprazole-treated *Vglut2*$^{f/f;CaMKII\text{-}Cre}$ mice and supports an effect of the targeted mutation on the dopamine system. We next subjected *Vglut2*$^{f/f;CaMKII\text{-}Cre}$ mice and littermate controls to amphetamine or 8-hydroxy-2-(di-*n*-propylmino)tetralin (8-OH-DPAT) treatments and analyzed their level of activity. Interestingly, amphetamine treatment, which affects the dopaminergic system via the dopamine transporter, significantly increased the activity of the *Vglut2*$^{f/f;CaMKII\text{-}Cre}$ mice compared with the controls (30%; $p <$ 0,01), whereas treatment with 8-OH-DPAT, a 5-HT$_{1A}$ receptor agonist, did not alter their total activity (Fig. 7). These results further strengthen the observation that the dopamine system is affected downstream of the *Vglut2* mutation.

Discussion

We generated a genetic mouse model with reduced VGLUT2-mediated neurotransmission by selective deletion of VGLUT2-mediated glutamatergic neurotransmission in CaMKIIα-specific areas of the forebrain. This model has unique properties, because it targets the presynaptic site of the glutamatergic synapse with late onset in the juvenile animal. Despite the restricted deletion of *Vglut2* in this model, the mice exhibit a prominent alteration in their behavior. The *Vglut2*$^{f/f;CaMKII\text{-}Cre}$ mice show reduced anxiety and increased locomotion in the elevated plus maze, a finding that was strongly corroborated by analysis in the MCSF. In contrast, we do not find impairments in depressive behavior measured by the Porsolt forced swim test, nor in learning or synaptic function in the dentate gyrus. In addition to the hyperlocomotion and blunted anxiety, the mice show impairments in spatial long-term memory and prepulse inhibition. The selective deletion of *Vglut2* expression in neurons of the cortical and amygdaloid areas is in all probability responsible for the observed altered behaviors in the *Vglut2*$^{f/f;CaMKII\text{-}Cre}$ mice.

VGLUT2 in neurocircuitry of higher brain function

To better understand the neurocircuitry responsible for the altered behavior in *Vglut2*$^{f/f;CaMKII\text{-}Cre}$ mice, we analyzed target areas of the neurons that had lost their *Vglut2* expression. The amygdaloid nuclei projecting to the striatum include the basolateral amygdaloid complex, the basomedial nucleus, the anterior and posterior cortical nucleus (Paxinos, 1994), of which the latter three express Vglut2 mRNA (Fig. 1). It is also known that the amygdala receives projections from the subiculum (Paxinos, 1994). The amygdala has been extensively linked to emotional behavior, and therefore, we find it likely that the emotional deficits observed in this study, including decreased anxiety and increased risk-taking, are linked to the lack of VGLUT2 either in terminals on the amygdala or in the glutamatergic neurons of the amygdala. The decreased anxiety observed in the *Vglut2*$^{f/f;CaMKII\text{-}Cre}$ mice is in contrast to a recent study, which demonstrated that heterozygous *Vglut1* animals are more anxious than control animals (Tordera et al., 2007), suggesting an interesting interplay between VGLUT1- and VGLUT2-mediated glutamatergic neurotransmission in anxiety-related behavior.

The loss of *Vglut2* expression in the subiculum is likely responsible for the reduction of VGLUT2-positive terminals in the nucleus accumbens, because it has been demonstrated that the subiculum is one of the major output regions of the hippocampus and thus project to many regions of the CNS including the cortex, the nucleus accumbens, and the amygdala (Paxinos, 1994). The observed decrease of VGLUT2-positive varicosities in the dorsolateral striatum may be connected to the removal of *Vglut2* in the RSG and/or the subicular/presubicular region (Figs. 1, 2). The afferent projections to the striatum originate from cortical areas including the allocortex, mesocortex (part of which is the subiculum and RSG), and neocortex (Paxinos, 1994). RSG projections terminate in the striatum, making it possible that the observed reduction of Vglut2-positive terminals originate in the RSG. The thalamus also project extensively to the striatum, but because we do not detect a decrease in the expression of thalamic Vglut2 mRNA levels, the reduction of terminals is not likely of a thalamic origin. The afferent projections to the striatum originate in several cortical areas including the allocortex, mesocortex (part of which is the subiculum and RSG), and neocortex, and it is likely that the Vglut2-expressing neurons found in these areas contribute to the reduced amount of VGLUT-positive terminals in the striatum. Also, because of the massive abundance of VGLUT2-

positive terminals in the adult brain and given the complexity in the behavioral phenotype of the *Vglut2*$^{f/f;CaMKII\text{-}Cre}$ mice, it is possible that our characterization of VGLUT2-containing terminals in target areas of the *Vglut2*-deleted neurons may have left certain changes undetected.

Although the deletion of *Vglut2* is here restricted to a limited number of neuronal populations, a full understanding of the neurons involved in generating the phenotype likely requires an even more restricted deletion. For example, it would be interesting to investigate whether a deletion of *Vglut2* in the cortical area, and not in the amygdala, would replicate the cognitive deficits but leave certain aspects of emotional behavior normal, and vice versa. Notably, the dorsolateral striatum and the nucleus accumbens, regions having lost a significant number of VGLUT2 terminals, are target areas of the nigrostriatal and mesolimbocortical dopaminergic pathways, both of which are involved in mediating spontaneous hyperlocomotion through an increase in dopaminergic tone (Giros et al., 1996).

Significant effect on dopaminergic components

It has been described that dopaminergic activity is modulated by glutamatergic projections from several areas including the cortex and the amygdala (Carlsson et al., 1999; Laruelle et al., 2003) and that glutamatergic afferents and dopaminergic projections converge on GABAergic striatal medial spiny neurons (Smith and Bolam, 1990). In addition to the indirect modulation of dopamine neuron activity via the medium spiny neurons, which has been suggested to act as a "break" on dopamine release, the cortical glutamatergic neurons have also been suggested to act as an "accelerator" on dopamine release through direct innervation of the dopamine neurons in the ventral tegmental area. The balance between the "break" and the "accelerator" accounts for the net effect on dopamine release (Carlsson et al., 2001). Interestingly, concomitant with the loss of VGLUT2-positive projections in *Vglut2*$^{f/f;CaMKII\text{-}Cre}$ mice, we observe a 70% increase in the striatal binding of the radiolabeled DRD2 agonist [^{11}C]raclopride (Fig. 6). This increase in binding is seen in naive mice (i.e., in the absence of any pharmacological challenge, such as amphetamine stimulation of dopamine release, or even reserpine stimulation for dopamine depletion), suggesting a rather profound effect on the dopamine system. However, the underlying mechanism for the increase in [^{11}C]raclopride binding is not yet known. Notably, [^{11}C]raclopride binding potential has been well documented as an indirect measure of changes in synaptic dopamine concentrations induced by challenge, and that a decrease in [^{11}C]raclopride binding is linked to increased dopamine occupancy on the dopamine D_2 receptors (Breier et al., 1997; Thanos et al., 2002; Piccini et al., 2003). The exact nature of such increased occupancy, whether it depends on direct competition for binding sites or a more complex noncompetitive mechanism, such as internalization of D_2 receptors, is currently debated and under investigation (Ginovart, 2005). By comparing our PET data with studies showing a direct link between decreased raclopride binding and increased dopamine binding at D_2 receptors, it may initially seem as the *Vglut2*$^{f/f;CaMKII\text{-}Cre}$ mice would have a lower degree of dopamine binding. Notably, the here presented genetically induced chronic downregulation of VGLUT2 could affect several aspects of synaptic function (e.g., the actual density of dopamine receptors). The observed increase in raclopride binding is thus more difficult to interpret and warrants additional *in vivo* investigations.

Several results from our study described here point to an increase in dopamine signaling in the *Vglut2*$^{f/f;CaMKII\text{-}Cre}$ mice. First, measurements of total tissue dopamine content showed significant increased levels in the striatum of mutant mice. Second, *Vglut2*$^{f/f;CaMKII\text{-}Cre}$ mice respond to administration of the partial dopamine D_2 receptor agonist aripiprazole by improvement of sensory filtering. Third, *Vglut2*$^{f/f;CaMKII\text{-}Cre}$ mice display an augmented response to amphetamine treatment demonstrated by an increase in locomotor activity. Glutamatergic as well as dopaminergic neurotransmission in the striatum is thus affected by the *Vglut2* mutation. Collectively, our results suggest that the neurocircuitry affected by the targeted deletion in the *Vglut2*$^{f/f;CaMKII\text{-}Cre}$ mice contains a midbrain dopaminergic component, and it is likely that the observed hyperlocomotion, and possibly also aspects of the social, cognitive, and emotional behavioral defects, are linked to a dysfunction in this system. The *Vglut2*$^{f/f;CaMKII\text{-}Cre}$ mouse model therefore links reduced VGLUT2-mediated neurotransmission to an altered dopaminergic activity, similar to the previously suggested hypoglutamatergic influence by data from pharmacological experiments and tracing studies (Kegeles et al., 2000; Sesack et al., 2003).

Is the *Vglut2*$^{f/f;CaMKII\text{-}Cre}$ phenotype of relevance for psychiatric disorder?

Apart from their increased social interaction, the phenotype of the *Vglut2*$^{f/f;CaMKII\text{-}Cre}$ mice relates to several phenotypes associated with animal models of schizophrenia (Powell and Miyakawa, 2006). Increased locomotor activity in response to novel environments, as seen both in the elevated plus maze and the concentric square field (Fig. 3), falls into the category of phenotypes that has been established for schizophrenia animal models to describe "positive symptoms." However, altered social dominance as detected in the social dominance test, and blunted emotional expression, as seen in the elevated plus maze and the MCSF, fit the criteria established for "negative symptoms," whereas impaired long-term spatial memory is a cognitive dysfunction (Fig. 4). Importantly, PPI, which can be used to analyze the ability of sensory filtering in human subjects, constitutes a translational measure well validated also for rodents. Using this method, we see a significant decrease in sensory filtering in the *Vglut2*$^{f/f;CaMKII\text{-}Cre}$ mice, a feature that is partially reversed by the partial D_2 agonist aripiprazole, a novel atypical antipsychotic drug that is used for treatment of schizophrenia (Burris et al., 2002).

Schizophrenia has been associated to dysfunction of glutamatergic neurotransmission involving NMDA receptors (Jentsch and Roth, 1999). Noncompetitive inhibitors of NMDA receptors, including PCP, ketamine, and MK-801 [(+)-5-methyl-10,11-dihydro-5*H*-dibenzo[a,d]cyclohepten-5,10-imine maleate], induce schizophrenia-form symptoms when systemically administrated in a normal individual and exacerbate these symptoms in schizophrenic patients (Krystal et al., 1994; Monyer et al., 1994; Lahti et al., 1995). In our study, PCP challenge did not seem to further disrupt the PPI response in *Vglut2*$^{f/f;CaMKII\text{-}Cre}$ mice (Fig. 4), indicating that no additional decrease of the filtering defect could be induced. This suggests either that the underlying mechanisms for a hypoglutamatergic response mediated by the NMDA receptor had been abolished or that the effect of a hypoglutamatergic state on PPI was saturated. Several genetic animal models have been produced, which suggest a role for altered glutamate neurotransmission in schizophrenia, including both mutations in glutamate receptor genes, and mutations in genes linked to schizophrenia in patients. For example, mice with reduced levels of the essential NR1 subunit showed schizophrenia-like behavioral characteristics, which could be restored with an-

tipsychotic drugs (Mohn et al., 1999). The observed downstream effects on the dopaminergic system in the *Vglut2*$^{f/f;CaMKII\text{-}Cre}$ mice may suggest that potential therapies targeting the glutamatergic system can be improved by striving for a subsequent influence on the dopaminergic system. Recently, strong support for a role of glutamate neurotransmission in schizophrenia came from the study of an oral prodrug of a selective agonist for metabotropic glutamate 2/3 receptors that had shown antipsychotic potential in animal studies. This compound was shown to ameliorate both positive and negative symptoms in schizophrenic patients in a comparable manner to clozapine (Patil et al., 2007).

It is well known that dopamine D_2 receptor antagonists have antipsychotic effects and that indirect agonists such as amphetamine can induce psychosis. Also, various experimental approaches using a combination of pharmacology and imaging by several laboratories have shown an increased dopamine release in response to amphetamine provocation in patients with schizophrenia compared with controls; in addition, baseline dopamine levels have also been shown to be increased in schizophrenia patients (Laruelle et al., 2005). However, as stated by Carlsson and colleagues, the elevation of dopamine release observed in patients with schizophrenia is not necessarily a primary phenomenon, but could be a consequence of, for example, hypoglutamatergia. In support of this, it has been found in both rats and humans that drugs that block NMDA receptors are capable of enhancing the spontaneous and especially the amphetamine-induced release of dopamine, by a mechanism that is not yet known (for review, see Carlsson et al., 2001). In this respect, it is interesting to note that *Vglut2*$^{f/f;CaMKII\text{-}Cre}$ mice are more sensitive to provocation with amphetamine than control littermates (Fig. 7) and to also analyze extracellular dopamine content and the kinetics of [^{11}C]raclopride occupancy in these mice after a similar provocation would be highly interesting. Although the behavior of *Vglut2*$^{f/f;CaMKII\text{-}Cre}$ mice manifests a schizophrenia-like phenotype, as established for animal models, it should be noted that it is not certain to what extent the observed behaviors of the mice is of actual relevance for schizophrenia. It is also important to keep in mind that the behavioral changes observed in the *Vglut2*$^{f/f;CaMKII\text{-}Cre}$ mice not necessarily all are connected to the regulation of dopamine levels; instead, they may be dependent on the loss of specific VGLUT2-mediated neurotransmisson itself.

The *Vglut2*$^{f/f;CaMKII\text{-}Cre}$ mouse could become an important research tool in drug-identifying endeavors, and importantly, because this mouse model downregulates glutamate release from the presynaptic site, it offers a unique opportunity to test drugs acting on postsynaptic targets, because the model does not confound the measurements by affecting this region of the synapse directly. In addition, the *Vglut2*$^{f/f;CaMKII\text{-}Cre}$ mice display a temporal expression pattern that may be of relevance to schizophrenia, a disorder in which symptoms often emerge at late adolescence. The reduced VGLUT2-mediated neurotransmission of the *Vglut2*$^{f/f;CaMKII\text{-}Cre}$ mice is induced at ~3 weeks of age, which notably, despite this restriction in time of onset, is sufficient to induce profound changes in behavior. In summary, we deleted *Vglut2* expression in neurons of the cortex, hippocampus, and amygdala, and identified a role for VGLUT2 in neuronal circuitry of higher brain functions including cognitive, social, and emotional behavior. Even with the restricted deletion of VGLUT2-mediated signaling in the *Vglut2*$^{f/f;CaMKII\text{-}Cre}$ mouse, the clear molecular and behavioral consequences of this deletion suggest that this genetic mouse model may become useful for additional studies of reduced VGLUT2-mediated neurotransmission in relation to higher brain function and disorders thereof.

References

Allen RM, Young SJ (1978) Phencyclidine-induced psychosis. Am J Psychiatry 135:1081–1084.

Arguello PA, Gogos JA (2006) Modeling madness in mice: one piece at a time. Neuron 52:179–196.

Bellocchio EE, Reimer RJ, Fremeau RT Jr, Edwards RH (2000) Uptake of glutamate into synaptic vesicles by an inorganic phosphate transporter. Science 289:957–960.

Breier A, Su TP, Saunders R, Carson RE, Kolachana BS, de Bartolomeis A, Weinberger DR, Weisenfeld N, Malhotra AK, Eckelman WC, Pickar D (1997) Schizophrenia is associated with elevated amphetamine-induced synaptic dopamine concentrations: evidence from a novel positron emission tomography method. Proc Natl Acad Sci U S A 94:2569–2574.

Burris KD, Molski TF, Xu C, Ryan E, Tottori K, Kikuchi T, Yocca FD, Molinoff PB (2002) Aripiprazole, a novel antipsychotic, is a high-affinity partial agonist at human dopamine D2 receptors. J Pharmacol Exp Ther 302:381–389.

Carlsson A, Hansson LO, Waters N, Carlsson ML (1999) A glutamatergic deficiency model of schizophrenia. Br J Psychiatry Suppl 1999:2–6.

Carlsson A, Waters N, Holm-Waters S, Tedroff J, Nilsson M, Carlsson ML (2001) Interactions between monoamines, glutamate, and GABA in schizophrenia: new evidence. Annu Rev Pharmacol Toxicol 41:237–260.

Ellenbroek BA, Sluyter F, Cools AR (2000) The role of genetic and early environmental factors in determining apomorphine susceptibility. Psychopharmacology (Berl) 148:124–131.

File SE (1980) The use of social interaction as a method for detecting anxiolytic activity of chlordiazepoxide-like drugs. J Neurosci Methods 2:219–238.

Fredriksson A, Eriksson P, Archer T (1997) MPTP-induced deficits in motor activity: neuroprotective effects of the spintrapping agent, alpha-phenyl-*tert*-butyl-nitrone (PBN). J Neural Transm 104:579–592.

Fremeau RT Jr, Troyer MD, Pahner I, Nygaard GO, Tran CH, Reimer RJ, Bellocchio EE, Fortin D, Storm-Mathisen J, Edwards RH (2001) The expression of vesicular glutamate transporters defines two classes of excitatory synapse. Neuron 31:247–260.

Fremeau RT Jr, Voglmaier S, Seal RP, Edwards RH (2004a) VGLUTs define subsets of excitatory neurons and suggest novel roles for glutamate. Trends Neurosci 27:98–103.

Fremeau RT Jr, Kam K, Qureshi T, Johnson J, Copenhagen DR, Storm-Mathisen J, Chaudhry FA, Nicoll RA, Edwards RH (2004b) Vesicular glutamate transporters 1 and 2 target to functionally distinct synaptic release sites. Science 304:1815–1819.

Gallagher M, Burwell R, Burchinal M (1993) Severity of spatial learning impairment in aging: development of a learning index for performance in the Morris water maze. Behav Neurosci 107:618–626.

Ginovart N (2005) Imaging the dopamine system with in vivo [^{11}C]raclopride displacement studies: understanding the true mechanism. Mol Imaging Biol 7:45–52.

Giros B, Jaber M, Jones SR, Wightman RM, Caron MG (1996) Hyperlocomotion and indifference to cocaine and amphetamine in mice lacking the dopamine transporter. Nature 379:606–612.

Gras C, Herzog E, Bellenchi GC, Bernard V, Ravassard P, Pohl M, Gasnier B, Giros B, El Mestikawy S (2002) A third vesicular glutamate transporter expressed by cholinergic and serotoninergic neurons. J Neurosci 22:5442–5451.

Haitina T, Takahashi A, Holmén L, Enberg J, Schiöth HB (2007) Further evidence for ancient role of ACTH peptides at melanocortin (MC) receptors; pharmacology of dogfish and lamprey peptides at dogfish MC receptors. Peptides 28:798–805.

Herzog E, Bellenchi GC, Gras C, Bernard V, Ravassard P, Bedet C, Gasnier B, Giros B, El Mestikawy S (2001) The existence of a second vesicular glutamate transporter specifies subpopulations of glutamatergic neurons. J Neurosci 21:RC181(1–6).

Hippenmeyer S, Vrieseling E, Sigrist M, Portmann T, Laengle C, Ladle DR, Arber S (2005) A developmental switch in the response of DRG neurons to ETS transcription factor signaling. PLoS Biol 3:e159.

Jentsch JD, Roth RH (1999) The neuropsychopharmacology of phencyclidine: from NMDA receptor hypofunction to the dopamine hypothesis of schizophrenia. Neuropsychopharmacology 20:201–225.

Kaneko T, Fujiyama F (2002) Complementary distribution of vesicular glutamate transporters in the central nervous system. Neurosci Res 42:243–250.

Kegeles LS, Abi-Dargham A, Zea-Ponce Y, Rodenhiser-Hill J, Mann JJ, Van Heertum RL, Cooper TB, Carlsson A, Laruelle M (2000) Modulation of amphetamine-induced striatal dopamine release by ketamine in humans: implications for schizophrenia. Biol Psychiatry 48:627–640.

Krystal JH, Karper LP, Seibyl JP, Freeman GK, Delaney R, Bremner JD, Heninger GR, Bowers MB Jr, Charney DS (1994) Subanesthetic effects of the noncompetitive NMDA antagonist, ketamine, in humans. Psychotomimetic, perceptual, cognitive, and neuroendocrine responses. Arch Gen Psychiatry 51:199–214.

Lagerström MC, Rabe N, Haitina T, Kalnina I, Hellström AR, Klovins J, Kullander K, Schiöth HB (2007) The evolutionary history and tissue mapping of GPR123: specific CNS expression pattern predominantly in thalamic nuclei and regions containing large pyramidal cells. J Neurochem 100:1129–1142.

Lahti AC, Koffel B, LaPorte D, Tamminga CA (1995) Subanesthetic doses of ketamine stimulate psychosis in schizophrenia. Neuropsychopharmacology 13:9–19.

Laruelle M, Kegeles LS, Abi-Dargham A (2003) Glutamate, dopamine, and schizophrenia: from pathophysiology to treatment. Ann N Y Acad Sci 1003:138–158.

Laruelle M, Frankle WG, Narendran R, Kegeles LS, Abi-Dargham A (2005) Mechanism of action of antipsychotic drugs: from dopamine D(2) receptor antagonism to glutamate NMDA facilitation. Clin Ther 27 [Suppl A]:S16–S24.

Lewis DA, Lieberman JA (2000) Catching up on schizophrenia: natural history and neurobiology. Neuron 28:325–334.

Lindblom J, Johansson A, Holmgren A, Grandin E, Nedergård C, Fredriksson R, Schiöth HB (2006) Increased mRNA levels of tyrosine hydroxylase and dopamine transporter in the VTA of male rats after chronic food restriction. Eur J Neurosci 23:180–186.

Lindzey G, Winston H, Manosevitz M (1961) Social dominance in inbred mouse strains. Nature 191:474–476.

Lobe CG, Koop KE, Kreppner W, Lomeli H, Gertsenstein M, Nagy A (1999) Z/AP, a double reporter for cre-mediated recombination. Dev Biol 208:281–292.

Luby ED, Cohen BD, Rosenbaum G, Gottlieb JS, Kelley R (1959) Study of a new schizophrenomimetic drug; sernyl. AMA Arch Neurol Psychiatry 81:363–369.

Meyerson BJ, Augustsson H, Berg M, Roman E (2006) The concentric square field: a multivariate test arena for analysis of explorative strategies. Behav Brain Res 168:100–113.

Minichiello L, Korte M, Wolfer D, Kühn R, Unsicker K, Cestari V, Rossi-Arnaud C, Lipp HP, Bonhoeffer T, Klein R (1999) Essential role for TrkB receptors in hippocampus-mediated learning. Neuron 24:401–414.

Moechars D, Weston MC, Leo S, Callaerts-Vegh Z, Goris I, Daneels G, Buist A, Cik M, van der Spek P, Kass S, Meert T, D'Hooge R, Rosenmund C, Hampson RM (2006) Vesicular glutamate transporter VGLUT2 expression levels control quantal size and neuropathic pain. J Neurosci 26:12055–12066.

Mohn AR, Gainetdinov RR, Caron MG, Koller BH (1999) Mice with reduced NMDA receptor expression display behaviors related to schizophrenia. Cell 98:427–436.

Monyer H, Burnashev N, Laurie DJ, Sakmann B, Seeburg PH (1994) Developmental and regional expression in the rat brain and functional properties of four NMDA receptors. Neuron 12:529–540.

Morris R (1984) Developments of a water-maze procedure for studying spatial learning in the rat. J Neurosci Methods 11:47–60.

Oliveira AL, Hydling F, Olsson E, Shi T, Edwards RH, Fujiyama F, Kaneko T, Hökfelt T, Cullheim S, Meister B (2003) Cellular localization of three vesicular glutamate transporter mRNAs and proteins in rat spinal cord and dorsal root ganglia. Synapse 50:117–129.

Patil ST, Zhang L, Martenyi F, Lowe SL, Jackson KA, Andreev BV, Avedisova AS, Bardenstein LM, Gurovich IY, Morozova MA, Mosolov SN, Neznanov NG, Reznik AM, Smulevich AB, Tochilov VA, Johnson BG, Monn JA, Schoepp DD (2007) Activation of mGlu2/3 receptors as a new approach to treat schizophrenia: a randomized phase 2 clinical trial. Nat Med 13:1102–1107.

Paxinos G (1994) The rat nervous system, Ed 2. San Diego: Academic.

Pellow S, Chopin P, File SE, Briley M (1985) Validation of open:closed arm entries in an elevated plus-maze as a measure of anxiety in the rat. J Neurosci Methods 14:149–167.

Piccini P, Pavese N, Brooks DJ (2003) Endogenous dopamine release after pharmacological challenges in Parkinson's disease. Ann Neurol 53:647–653.

Porsolt RD, Le Pichon M, Jalfre M (1977) Depression: a new animal model sensitive to antidepressant treatments. Nature 266:730–732.

Powell CM, Miyakawa T (2006) Schizophrenia-relevant behavioral testing in rodent models: a uniquely human disorder? Biol Psychiatry 59:1198–1207.

Roman E, Ploj K, Gustafsson L, Meyerson BJ, Nylander I (2006) Variations in opioid peptide levels during the estrous cycle in Sprague-Dawley rats. Neuropeptides 40:195–206.

Sakata-Haga H, Kanemoto M, Maruyama D, Hoshi K, Mogi K, Narita M, Okado N, Ikeda Y, Nogami H, Fukui Y, Kojima I, Takeda J, Hisano S (2001) Differential localization and colocalization of two neuron-types of sodium-dependent inorganic phosphate cotransporters in rat forebrain. Brain Res 902:143–155.

Seeman P, Lee T, Chau-Wong M, Wong K (1976) Antipsychotic drug doses and neuroleptic/dopamine receptors. Nature 261:717–719.

Sesack SR, Carr DB, Omelchenko N, Pinto A (2003) Anatomical substrates for glutamate-dopamine interactions: evidence for specificity of connections and extrasynaptic actions. Ann N Y Acad Sci 1003:36–52.

Smith AD, Bolam JP (1990) The neural network of the basal ganglia as revealed by the study of synaptic connections of identified neurones. Trends Neurosci 13:259–265.

Stornetta RL, Sevigny CP, Schreihofer AM, Rosin DL, Guyenet PG (2002) Vesicular glutamate transporter DNPI/VGLUT2 is expressed by both C1 adrenergic and nonaminergic presympathetic vasomotor neurons of the rat medulla. J Comp Neurol 444:207–220.

Swerdlow NR, Geyer MA (1998) Using an animal model of deficient sensorimotor gating to study the pathophysiology and new treatments of schizophrenia. Schizophr Bull 24:285–301.

Takamori S, Rhee JS, Rosenmund C, Jahn R (2000) Identification of a vesicular glutamate transporter that defines a glutamatergic phenotype in neurons. Nature 407:189–194.

Takamori S, Rhee JS, Rosenmund C, Jahn R (2001) Identification of differentiation-associated brain-specific phosphate transporter as a second vesicular glutamate transporter (VGLUT2). J Neurosci 21:RC182(1–6).

Tamminga CA, Holcomb HH (2005) Phenotype of schizophrenia: a review and formulation. Mol Psychiatry 10:27–39.

Thanos PK, Taintor NB, Alexoff D, Vaska P, Logan J, Grandy DK, Fang Y, Lee JH, Fowler JS, Volkow ND, Rubinstein M (2002) In vivo comparative imaging of dopamine D2 knockout and wild-type mice with ^{11}C-raclopride and microPET. J Nucl Med 43:1570–1577.

Tordera RM, Totterdell S, Wojcik SM, Brose N, Elizalde N, Lasheras B, Del Rio J (2007) Enhanced anxiety, depressive-like behaviour and impaired recognition memory in mice with reduced expression of the vesicular glutamate transporter 1 (VGLUT1). Eur J Neurosci 25:281–290.

Tronche F, Kellendonk C, Kretz O, Gass P, Anlag K, Orban PC, Bock R, Klein R, Schütz G (1999) Disruption of the glucocorticoid receptor gene in the nervous system results in reduced anxiety. Nat Genet 23:99–103.

Varoqui H, Schäfer MK, Zhu H, Weihe E, Erickson JD (2002) Identification of the differentiation-associated Na^+/PI transporter as a novel vesicular glutamate transporter expressed in a distinct set of glutamatergic synapses. J Neurosci 22:142–155.

Wallén-Mackenzie A, Gezelius H, Thoby-Brisson M, Nygård A, Enjin A, Fujiyama F, Fortin G, Kullander K (2006) Vesicular glutamate transporter 2 is required for central respiratory rhythm generation but not for locomotor central pattern generation. J Neurosci 26:12294–12307.

Wojcik SM, Rhee JS, Herzog E, Sigler A, Jahn R, Takamori S, Brose N, Rosenmund C (2004) An essential role for vesicular glutamate transporter 1 (VGLUT1) in postnatal development and control of quantal size. Proc Natl Acad Sci U S A 101:7158–7163.